Algal Research 99 (2026) 104937

Contents lists available at ScienceDirect

Algal Research

journal homepage: www.elsevier.com/locate/algal

Integrating a combinatorial structure database and feature-based molecular networking to identify mycosporine-like amino acids in the aerophytic green alga *Apatococcus ammoniophilus*

Fabian Hammerle [a,*], Ulrik Søchting [b], Armin Oberosler [a], Cornelia A. Karg [a], Michael J. Zwerger [c], Christina Stöckholzer [a], Stefan Schwaiger [a], Ursula Peintner [d], Johanna M. Gostner [e,f], Ulf Karsten [g,h], Markus Ganzera [a]

[a] Institute of Pharmacy, Department of Pharmacognosy, University of Innsbruck, Innrain 80-82, 6020, Innsbruck, Austria
[b] Section Ecology and Evolution, Department of Biology, University of Copenhagen, Universitetsparken 15, 2100, Copenhagen, Denmark
[c] Institute of Analytical Chemistry and Radiochemistry, University of Innsbruck, Innrain 80-82, 6020, Innsbruck, Austria
[d] Department of Microbiology, University of Innsbruck, Technikerstraße 25, 6020, Innsbruck, Austria
[e] Institute of Medical Biochemistry, Medical University of Innsbruck, Innrain 80, 6020, Innsbruck, Austria
[f] Core Facility Metabolomics II, Medical University of Innsbruck, Innrain 80, 6020, Innsbruck, Austria
[g] Department of Applied Ecology and Phycology, Institute of Biological Sciences, University of Rostock, Albert-Einstein-Straße 3, 18051, Rostock, Germany
[h] Interdisciplinary Faculty, Department of Maritime Systems, University of Rostock, Albert-Einstein-Straße 21, 18051, Rostock, Germany

ARTICLE INFO

Keywords:
Trebouxiophyceae
Mycosporine-like amino acid
Metabolomics
Feature-based molecular networking
Sunscreen

ABSTRACT

Apatococcus ammoniophilus (Trebouxiophyceae) is a recently identified green alga forming green biofilms on the bark and twigs of coniferous trees. It contains high amounts of an unknown mycosporine-like amino acid (MAA), a compound class known for its photoprotective, antioxidant, and wound-healing properties. To identify this MAA, a workflow combining UHPLC-VWD-HRMS^2 analysis, feature-based molecular networking, and metabolite annotation using a rationally designed combinatorial database was developed. By leveraging the limited set of known MAA core structures and amino acid-related substituents, a theoretical compound library was created in silico and implemented into the bioinformatics platform SIRIUS. Applying the workflow to various extracts of *A. ammoniophilus* and the basidiomycete *Stereum gausapatum*, included as an MAA-producing reference to test whether both organisms share the same unknown MAA, enabled the putative annotation of several MAA candidates and led to the isolation, structure elucidation, and biological activity evaluation of three compounds: mycosporine-serinol, gadusol, and the novel algasporine-glycine. Overall, this study provides valuable insights into the variable MAA profile of an aerophytic microalga, highlighting its potential for future biotechnological applications in studying photoprotection in terrestrial organisms, while also establishing a broadly applicable workflow for the discovery and annotation of MAAs in natural extracts.

1. Introduction

Apatococcus ammoniophilus Søchting, Friedl & Moestrup is a recently described aerophytic filamentous green alga within the class Trebouxiophyceae, notable for its ability to form dense, light green mats on the bark, twigs, and needles of primarily coniferous trees (Fig. 1A-C) [1]. Morphologically, *A. ammoniophilus* consists of unbranched filaments (Fig. 1C) composed of characteristic two-celled units, each containing a flat, lobed chloroplast with a central nucleus surrounded by a distinctive ring of small particles, a feature unique to the genus *Apatococcus*. The thick-walled cells often contain storage oil droplets between the chloroplast and the cell wall, and they lack pyrenoids, which distinguishes them from morphologically similar taxa [1]. Biochemically, *A. ammoniophilus* exhibits remarkable adaptive traits to aeroterrestrial life, including high intracellular concentrations of the protective polyol erythritol and the presence of a unique UV-absorbing mycosporine-like amino acid (MAA). These compounds are thought to contribute to its resilience under desiccation stress and strong solar irradiation, respectively. In recent decades, this green alga has rapidly expanded across Denmark, northern Europe, and the British Isles, particularly in humid

* Corresponding author.
E-mail address: fabian.hammerle@uibk.ac.at (F. Hammerle).

https://doi.org/10.1016/j.algal.2026.104937
Received 19 February 2026; Received in revised form 27 July 2026; Accepted 22 August 2026
Available online 24 August 2026

regions with cool climates and elevated atmospheric nitrogen deposition, a pattern that correlates with intensive agricultural activity [1]. Its invasive colonization of Christmas tree plantations causes visible discoloration of the needles and hence considerable economic losses. Furthermore, the pronounced affinity of *A. ammoniophilus* for ammonia-rich environments suggests that it may serve as a valuable bioindicator of environmental nitrogen pollution, highlighting its ecological importance.

The biosynthesis and accumulation of MAAs represents a key photoprotective strategy that has evolved in numerous terrestrial and aquatic organisms to mitigate the damaging effects of ultraviolet radiation (UVR). MAAs are small, water-soluble metabolites derived from non-aromatic cyclohexenone or cyclohexenimine core structures substituted with amino acids or their corresponding amino alcohols. Structural variants have also been reported from other terrestrial green algae, such as streptophycean *Klebsormidium* species [2] and members of the Prasiolaceae (Trebouxiophyceae) [3], including klebsormidin A and B, which feature a gadusol scaffold substituted with an amino acid and an *N*-methyl group. More than 70 MAAs have been identified to date [4], differing mainly in their amino acid substituents. They are biosynthesized via the shikimate and/or pentose phosphate pathways [5–7] and function as natural sunscreens by absorbing UVR. Besides their protective role in the producing organisms, MAAs are transferred across trophic levels and accumulate in higher organisms, including marine invertebrates such as sea urchins, corals or sponges, and even fish [8–10]. In fish, MAAs are found at elevated levels in particularly UV-sensitive tissues such as the gonads (e.g., ripe eggs [11]) and the eyes [12–14]. Given their established UV-absorbing properties, this tissue-specific distribution in fish is hypothesized to contribute to protection against UV-induced damage.

MAAs possess very high molar extinction coefficients ($\varepsilon = 28{,}100$ to $50{,}000\ M^{-1}\ cm^{-1}$) and strong absorption between 310 and 360 nm, making them highly effective natural sunscreen compounds [15]. Their photoprotective efficiency is strongly influenced by water, which induces a bathochromic shift of their absorption maxima from the UV-B (280–315 nm) to the UV-A region (315–400 nm), the most abundant UVR reaching the Earth's surface. This shift results from enhanced intramolecular π-conjugation and the zwitterionic nature of the amino acid substituents. Recent ultrafast spectroscopic studies have shown that MAAs such as porphyra-334 dissipates absorbed UV energy through a

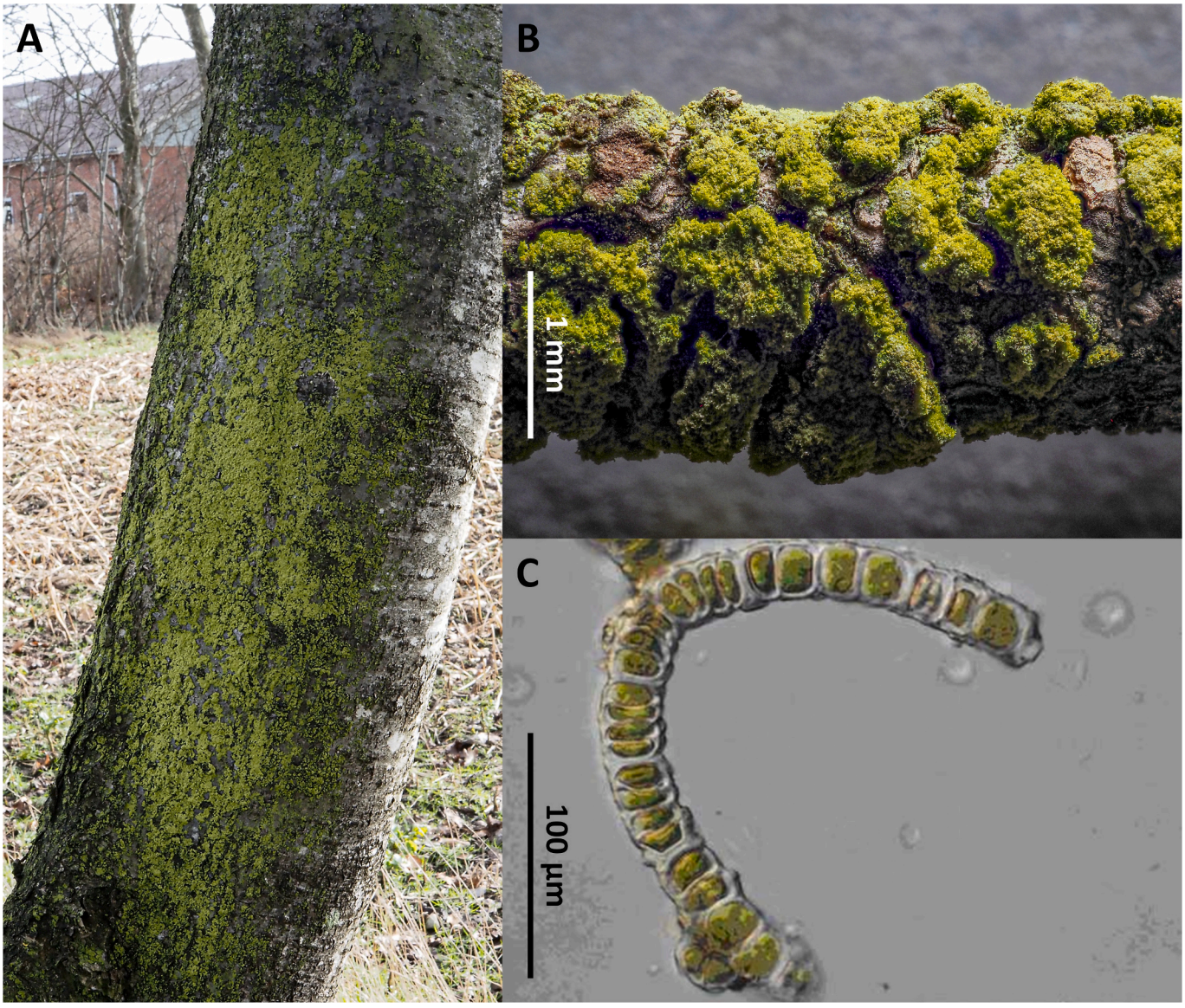

Fig. 1. A | *Apatococcus ammoniophilus* growing on *Scandosorbus intermedia* (Søchting #12947). B | Dry mat of hyphae on the upper side of a pine twig (Søchting #13044). C | Single *A. ammoniophilus* filament in water.

rapid non-radiative decay process referred to as the "button-on-a-string" mechanism. After UV excitation in aqueous environments, the cyclohexenimine ring rotates while maintaining hydrogen bonds with surrounding water molecules, allowing the absorbed energy to be released as heat within several hundred femtoseconds without bond cleavage or fluorescence emission [16].

In addition to photoprotection, a range of other physiological roles have been attributed to MAAs in cyanobacteria and algae, highlighting their potential function as multipurpose secondary metabolites [17,18]. For instance, they have been proposed to act as nitrogen storage compounds, either releasing nitrogen when required [19] or incorporating it under conditions of elevated ammonium availability. As an example, MAA accumulation has been observed in the red alga *Porphyra columbina* under combined exposure to ammonium and UVR [20]. Their concentrations have also been shown to respond to desiccation stress, potentially contributing to cellular protection through alterations of the cell matrix [21], and to increase under elevated temperatures [22]. Other properties ascribed to MAAs in the literature remain largely speculative. For example, their presumed role in maintaining osmotic balance in hypersaline environments [23] seems unlikely given their generally low abundance [15,24], while their alleged involvement in photosynthesis through energy transfer to chlorophyll [17,25] is questionable due to their weak fluorescence.

Over the past decades, research has not only focused on elucidating the ecological roles and bioactivities of MAAs in greater detail [15,26–29] but also on exploring their molecular diversity in natural sources. On the one hand, the so-called standard MAAs, including shinorine, palythine, asterina-330, and porphyra-334 among others, are widely distributed among macroalgae [30–32]. On the other hand, structurally unique variants such as the bostrychines appear to be restricted to the red algal genus *Bostrychia* [33–35]. To the best of our knowledge, however, with the exception of these compounds, no genuinely new MAA structure has been described in recent years. This is surprising, knowing the growing analytical [36,37] and computational capabilities [38] available today.

At the same time, phytochemical research has undergone a major transformation from traditional techniques to contextualized metabolomics [39]. High-resolution tandem mass spectrometry ($HRMS^2$) coupled with ultra-high-performance liquid chromatography (UHPLC) has become a standard analytical platform, while data-driven workflows increasingly shape modern natural product discovery. Bioinformatic approaches such as feature-based molecular networking [40] and its successor ion identity molecular networking [41] enable the evaluation of spectral similarities as well as their visualization, thereby reorganizing large MS^2 datasets into molecular families and making them accessible for exploration. The use of different similarity scoring methods, including the calculation of (modified) cosine scores or even artificial intelligence algorithms such as DreaMS [42] and MS2DeepScore [43], further enhance the structural clustering of related features. Individual compounds can be annotated with high confidence by integrating experimental data with in silico prediction tools such as SIRIUS [44] or tima ("taxonomically-informed metabolite annotation") [45]. Nevertheless, the lack of high-quality reference spectra for MAAs remains a major bottleneck. Apart from the GNPS (Global Natural Products Social Molecular Networking) community library [46], which also includes data contributed by our group, no large dedicated database for the comparison or annotation of MAAs is currently available. While GNPS and also GNPS2 [46], which contain resources such as MSnLib [47], have greatly expanded the accessibility of spectral data in general, MAAs remain underrepresented within these repositories. Consequently, advancing the molecular characterization of MAAs still depends largely on the acquisition of new experimental reference spectra and the continuous curation of publicly accessible datasets. Therefore, we hypothesized that the MAA building blocks described in the literature could be utilized to develop a specialized database that can be integrated into existing compound-annotation workflows, thereby facilitating the identification of unknown MAAs.

The present study pursued two main objectives. First, we aimed to isolate and structurally elucidate the previously reported MAA candidate from *A. ammoniophilus* [1], tentatively assigned as mycosporine-serine. This was required, as previous reports relied exclusively on UV/Vis and mass spectrometric data without definitive structural confirmation. To address this question, the basidiomycete *Stereum gausapatum* (Fr.) Fr., a local relative of *S. hirsutum* in which mycosporine-serine has been described [48], was collected and its MAA profile compared to that of *A. ammoniophilus*. In addition, the cytotoxicity and anti-oxidative effects of isolated compounds were tested in a human skin keratinocyte cell model to assess their photoprotective potential. Second, we pursued the development of an innovative and complementary approach for the annotation of experimental MS^2 spectra of putative MAAs. Following the concept of Nothias-Esposito et al. [49], we generated a combinatorial in silico MAA database compatible with the bioinformatic software SIRIUS. *S. gausapatum* and *A. ammoniophilus* were subjected to comprehensive chemical analysis, and their major MAAs isolated using a combination of chromatographic techniques. Structural suggestions were generated with the new combinatorial database and confirmed (using pure compounds) by 1D and 2D NMR spectroscopy. The database then was applied to screen the MAA profiles of several *A. ammoniophilus* samples collected across Denmark [1].

2. Materials and methods

2.1. Chemicals and solvents

Solvents were purchased from VWR International (Vienna, Austria) if not stated otherwise. Materials for liquid chromatography, 2′,7′-dichlorodihydrofluorescein diacetate (DCFH-DA), 2,2′-azobis(2-amidinopropane) dihydrochloride (AAPH), and Roswell Park Memorial Institute's medium (RPMI) were obtained from Merck (Darmstadt, Germany). Fetal bovine serum (FBS) was from Life Technologies (Darmstadt, Germany). MS-grade formic acid and ammonium formate came from VWR (Vienna, Austria) and Serva (Heidelberg, Germany), respectively. Ultra-pure water was produced using an Arium 611 UV system (Sartorius, Göttingen, Germany). Sephadex LH-20 material was purchased from GE Healthcare (Uppsala, Sweden).

2.2. General instrumentation

Samples were ground using a Bosch MKM 6003 grinder (Stuttgart, Germany), and extraction was performed in a Sonorex TK 52 ultrasonic bath (Bandelin, Berlin, Germany). A LABOROTA 4000 rotary evaporator (Heidolph, Schwabach, Germany) was used for evaporation and freeze-drying was conducted in a Benchtop Pro (SP Scientific, Warminster, PA, USA). For centrifugation, a Labofuge 400 (Heraeus, Hanau, Germany) or a Centrifuge 5804R (Eppendorf, Hamburg, Germany) were used; for mixing, a Vortex-Genie 2 (Scientific Industries, NY, USA). Reversed-phase medium-pressure liquid chromatography (RP-MPLC) separations were performed using a Reveleris® X2 system (BÜCHI, Flawil, Switzerland), equipped with a binary pump, an autosampler, an automated fraction collector, and an evaporative light-scattering as well as UV detector. Semi-preparative HPLC was carried out on an Agilent Technologies 1260 Infinity II system (Santa Clara, CA, USA) consisting of a quaternary pump (G7157A), a column oven (G7116A), a variable wavelength detector (G7114A), and a fraction collector (G1364F9). Volumes were transferred with pipettes and tips from Eppendorf. NMR experiments were conducted on spectrometers from Bruker (Karlsruhe, Germany): 700 MHz Avance 4 Neo (^{1}H: 700.20 MHz) and 400 MHz Avance 4 Neo (^{1}H: 400.13 MHz; ^{13}C: 100.62 MHz). Spectra were recorded in deuterated DMSO (DMSO-d_6, δ_H 2.50 ppm, δ_C 39.52 ppm) purchased from Euriso-Top (Cambridge Isotope Laboratories, Saint-Aubin, France). Pictures of thin-layer chromatographic analyses were taken with a Camag Reprostar 3 and edited with the software winCATS

(CAMAG, Muttenz, Switzerland). Any other specific instruments are mentioned in the respective chapters.

2.3. Origin of biomaterial, sample preparation, and isolation of MAAs

Fruiting bodies of *Stereum gausapatum* (Fr.) Fr. were collected by Ursula Peintner on the 13th October 2023 in South Tyrol (Montiglersee, Eppan, Italy). A taxonomic classification was achieved by evaluation of macroscopic and microscopic features. After collection, the biomaterial was dried at 50 °C in a desiccator. Voucher specimens are deposited at the Tyrolean State Museum Ferdinandeum with the collection number IBF20230683.

Apatococcus ammoniophilus growing in monospecific mats was collected from the bark of *Scandosorbus intermedia* in Jutland (Denmark) [1]. The material was air dried and kept at room temperature until extraction. The biomaterial used for the screening study is listed in the supplementary material and corresponds to that used in our previous study [1]. Samples were collected from different regions across Denmark to include geographically diverse material and comprised bark, twig, branch, and needle samples, predominantly from pine trees.

MAAs were isolated from polar extracts and fractions of *S. gausapatum* and *A. ammoniophilus* using a combination of different chromatographic techniques. Detailed experimental protocols can be found in the supplementary material.

2.4. Untargeted metabolomics analysis by UHPLC-VWD-ESI-HRMS^2 and feature-based molecular networking

For the structural annotation of the two MAAs present in *A. ammoniophilus* and *S. gausapatum*, a series of fractions containing reference compounds including shinorine, palythine, asterina-330, porphyra-334, aplysiapalythine A, mycosporine-glycine-alanine, aplysiapalythine B, mycosporine-methylamine-threonine, usujirene, and palythene were analyzed. Some of them originated from a previous study [34], while the remaining ones were obtained in the present work, including the *A. ammoniophilus* water extract and the *S. gausapatum* aqueous methanolic extract, each prepared at a concentration of 5 mg mL^{-1} in HPLC-grade water. Besides, extracts from the screening study and corresponding blanks were also analyzed.

Analyses were performed according to methods established in-house [10,38] on a Vanquish system (Thermo Scientific, Waltham, MA, USA) consisting of a binary pump (VC-P10-A), an autosampler (VC-A12-A), a column oven (VC-C10-A), and a variable wavelength detector (VC-D40-A) connected to a Thermo Scientific Exploris 120 Orbitrap HRMS unit. A Luna Omega C18 100 Å column (100 mm × 2.1 mm; particle size: 1.6 µm; Phenomenex, Torrance, CA, USA), protected by a SecurityGuard ULTRA guard C18 pre-column, served as stationary phase. The mobile phase comprised water with 0.25% formic acid and 20 mM ammonium formate (A) and acetonitrile (B). The applied gradient was as follows: 0 min, 0% B; 10 min, 5% B; 11 min, 90% B; 13 min, 90% B. Finally, the column was re-equilibrated with the original solvent composition (i.e., 0% B) for 20 min, which corresponds to a total run time of 33 min. The flow rate, column oven temperature, auto-sampler temperature, and injection volume were adjusted to 0.3 mL min^{-1}, 17 °C, 20 °C, and 1 µL, respectively. The detection wavelengths were set to 330 and 350 nm, the data collection rate to 2.0 Hz, the response time to 2.0 s, and the peak width to 0.2 min. Due to column aging, slight deviations in retention times were observed for some metabolites, including algasporine-glycine (first study: ID 1095, RT = 4.06 min; second study: ID 520, RT = 3.84 min).

The system was controlled by Thermo Scientific Xcalibur 4.4 software. Calibration of the mass analyzer was done via the Thermo Scientific proprietary calibration mix and the respective automatic calibration function. The mass spectrometric parameters were as follows: heated-ESI source, static spray voltage (positive: 3500 V), sheath gas (N_2): 30 arbitrary units, auxiliary gas (N_2): 17 arbitrary units, sweep gas (N_2): 0 arbitrary units. Temperature of the ion transfer tube and vaporizer was adjusted to 370 and 420 °C, respectively. MS data (range 70–1000 *m/z*) were recorded from 0 to 20 min with a resolution of 60,000 FWHM for MS^1. The RF lens parameter was set to 70%. Data-dependent experiments were conducted with stepped collision energy mode and normalized collision energy type using HCD collision energies of 15, 30, and 45% at a resolution of 15,000 FWHM. The number of dependent scans was set to 3. The following selection of filters was employed: intensity threshold filter (1.0E^5), dynamic exclusion (auto), isotope exclusion (assigned), charge state (perform dependent scans on singly charged precursors only), and apex filter (desired apex window: 75%). In addition, a specific exclusion list was created for the measurement using HPLC-grade water as a background extract with an IODA Mass Spec notebook [50].

Raw data were converted using MSConvert [51] and subsequently processed in mzmine (4.5.37 or 4.7.8) (mzio GmbH, Bremen, Germany) [52] before submission to the feature-based molecular networking (FBMN) workflow on GNPS (https://gnps.ucsd.edu/ProteoSAFe/static/gnps-splash.jsp) or GNPS2 (https://gnps2.org/homepage) [46] for molecular network creation [40]. Links to the publicly available FBMN jobs on GNPS and GNPS2 are included in the supplementary material. The DreaMS network was created using the Spectral / Molecular Networking function within mzmine with the following settings: merge & select fragment scans, merged (simple); presets, single scan: merged across energies; merging *m/z* tolerance: 0.0030 *m/z* or 10.0 ppm; min similarity: 60%; k-nearest neighbors, num. neighbors = 3, min neighbour similarity = 60%; batch size, 32 [42]. All molecular networks were visualized using Cytoscape software [53]. Detailed parameters for data processing and annotation are provided in the supplementary material.

2.5. Generating a combinatorial MAA database with SmiLib

The combinatorial MAA database was generated with SmiLib v2.0, which is a free, platform independent software tool [54] that can be downloaded from http://melolab.org/smilib/. As scaffolds, the different MAA core structures known in the literature were entered as SMILES code, including the cyclohexenone- (O=C1C(OC)=C(N[R1])CC(CO)(O)C1), the aminocyclohexenimine- (COC1=C(N[R1])CC(CO)(O)CC1=N[R2]), the klebsormidin- (O=C1C(OC)=C(CC(O)(C1O)CO)N(C)[R1]; later on called the algasporine-type), and the klebsormidin-type without the hydroxyl-group in position 4 (O=C1C(OC)=C(N([R1])C)CC(C1)(CO)O; deoxyalgasporine-type). The linker was defined as [A][R1]. Subsequently, several native and decarboxylated proteinogenic as well as non-proteinogenic amino acids were entered in the field "building blocks" (e.g., arginine: [A]C(CCCNC(N)=N)C(O)=O, arginine-CO2: [A]CCCCNC(N)=N). Defining an [A]H building block is not possible, as the output from SmiLib cannot be interpreted in the subsequent conversion step. This limitation also underlies the selection of the MAA core structures and the design of the input. The complete enumerated library was then saved as .txt file and used as input for the OPENBABEL chemical file format converter (https://www.cheminfo.org/Chemistry/Cheminformatics/FormatConverter/index.html) to change the SMILES code representation. The new list was then saved as .tsv file and finally a list of MAAs known from literature, to cover those with *H*-substitution like palythine, was added. This comprehensive list was then used to generate a SIRIUS-compatible combinatorial MAA database, comprising 4594 compounds with 1233 distinct molecular formulas, using the dedicated "Import Custom Databases" function in SIRIUS [44].

2.6. SIRIUS metabolite annotation

Metabolite annotation was performed with SIRIUS 6.1.1 [44,55,56]. The corresponding .mgf file was exported from mzmine (4.5.37 or 4.7.8) and subsequently processed. The parameters were set as follows: instrument, Orbitrap; MS^2 mass accuracy, 10 ppm; fix formula for detected lipid, yes; fallback adducts: $[M + H]^+$, $[M + Na]^+$, $[M + K]^+$; molecular

formula generation, de novo + bottom up). Molecular formula ranking was improved using ZODIAC [57]. The prediction of fingerprints was carried out with CSI:FingerID and the prediction of chemical classes with CANOPUS [56]. Only the combinatorial MAA database was searched for molecular structures, however, PubChem was allowed as fallback (confidence mode, approximate). Details on the overall annotation levels of the tentatively identified compounds are provided in the supplementary material.

2.7. Antioxidative activity and cytotoxicity testing of isolated MAAs

Human keratinocyte HaCaT cells (Cell Lines Service, Eppelheim, Germany) were used to evaluate the antioxidative activity and cytotoxicity of isolated MAAs. Cells were seeded at 2×10^4 cells per well (100 μL per well in Roswell Park Memorial Institute (RPMI) medium supplemented with 10% (*v*/v) fetal bovine serum (FBS)) in 96-well plates and incubated for 24 h at 37 °C in a humidified atmosphere containing 5% CO_2. Antioxidative activity was measured as reported previously [58], with minor modifications. Test compounds were prepared as stock solutions and serially diluted in Hanks' Balanced Salt Solution (HBSS). After incubation, the culture medium was removed and cells were washed once with 100 μL prewarmed HBSS. Cells were then incubated with 50 μL prewarmed HBSS containing 25 μM 2′,7′-dichlorodihydrofluorescein diacetate (DCFH-DA) and 50 μL HBSS (untreated control), compound dilution, or vehicle (vh) control (water). Plates were incubated for 1 h at 37 °C in the dark to allow intracellular probe loading. Thereafter, cells were washed once with prewarmed HBSS. Oxidative stress was induced by treatment with 600 μM freshly prepared 2,2′-azobis(2-amidinopropane) dihydrochloride (AAPH). Plates were incubated for 45 min at 37 °C, and intracellular reactive oxygen species (ROS) formation was quantified by measuring the fluorescence of oxidized dichlorofluorescein (DCF) at an excitation/emission wavelength of 485/535 nm using a Tecan Infinite F200 PRO microplate reader (Männedorf, Switzerland). After the measurement, HBSS was removed and 50 μL of growth medium containing 10% (*v*/v) CellTiter-Blue® reagent (Promega, Mannheim, Germany) was added to each well. Cells were incubated for 2 h at 37 °C in the dark. Cell viability was assessed based on the metabolic conversion of resazurin to resorufin, and fluorescence was measured at an excitation/emission wavelength of 560/600 nm. Four independent biological experiments, each performed with three technical replicates, were carried out. Statistical analyses were performed using GraphPad Prism 10.1.0 (GraphPad Software, San Diego, CA, USA). Differences between multiple groups were evaluated using one-way analysis of variance (ANOVA), followed by Dunnett's post hoc test for multiple comparisons against the respective control group. A p value <0.05 was considered statistically significant.

3. Results and discussion

3.1. Study overview

To identify the major unknown MAA in *A. ammoniophilus* and to characterize its overall MAA profile, we combined targeted extraction and chromatographic fractionation with untargeted metabolomics. Aqueous and aqueous methanolic extracts of *A. ammoniophilus* and *S. gausapatum*, together with a panel of reference MAAs, were analyzed by UHPLC-VWD-HRMS^2 and data were processed using mzmine [52], followed by feature-based molecular networking [40] to organize unique MS^2 spectra into clusters of structurally similar compounds. A combinatorial in silico MAA database was then constructed from known core scaffolds and amino acid substituents, implemented in SIRIUS [44], and used together with CANOPUS- [56] and ZODIAC-assisted [57] workflows to prioritize candidate structures for MAA-like features. Guided by these annotations, selected fractions were subjected to RP-MPLC, semi-preparative RP-HPLC, and semi-preparative HILIC for isolation, and the structures of the main MAAs, including the novel algasporine-glycine from *A. ammoniophilus* and mycosporine-serinol from *S. gausapatum*, were confirmed by 1D/2D NMR and MS^2 fragmentation analysis. Finally, we applied the combinatorial database-assisted annotation strategy to characterize the MAA profiles of multiple Danish *A. ammoniophilus* field samples. In parallel, gadusol and algasporine-glycine were quantified by HPLC-DAD, and the antioxidative capacity and cytotoxicity of the isolated MAAs assessed in HaCaT keratinocytes.

3.2. Chromatographic profiling of Stereum gausapatum and Apatococcus ammoniophilus extracts

In our previous study, we analyzed the aqueous extract of *A. ammoniophilus* and detected a potentially novel MAA different from prasiolin [3], which is characteristic for Trebouxiophyceae (Chlorophyta). Comprehensive (U)HPLC-VWD-MS^2 analyses revealed that this compound possesses the molecular formula $C_{11}H_{17}NO_7$ and an MS^2 fragmentation pattern theoretically consistent with that of mycosporine-serine [1]. In this study, *A. ammoniophilus* was re-investigated based on an increased amount of available biomaterial, allowing the preparative-scale isolation and subsequent structural characterization. The online UV/Vis spectrum exhibited a minor absorption peak at 224 nm and a pronounced absorption band at 324 nm. However, neither the chromatographic retention time nor the exact masses of the $[M + H]^+$ (*m/z* 276.1073) and $[2\,M + Na]^+$ (*m/z* 573.1896) ions corresponded to any of the available in-house MAA reference compounds (Fig. 2A-C). Furthermore, the MAA detected in the aqueous methanolic extract of *S. gausapatum*, a basidiomycete hypothesized to contain mycosporine-serine due to its close phylogenetic relationship to the only known biological source of this compound [48], displayed exact masses of *m/z* 262.1281 ($[M + H]^+$) and *m/z* 545.2315 ($[2\,M + Na]^+$) (Fig. 2B), indicating the presence of another entirely different compound. With a retention time of 2.40 min, the compound eluted slightly later than the widely distributed MAA porphyra-334, which showed a retention time of 2.33 min in the UHPLC analysis (Fig. 2A).

3.3. Combinatorial MAA database construction

Since MAAs are known to be highly hydrophilic and thus can only be extracted with polar solvents such as methanol or water, their purification is a labor-intensive process [59]. This includes the evaporation of large solvent volumes (of mostly water) or time-consuming steps like lyophilization. Therefore, our goal was to achieve a targeted and efficient isolation of the unknown compounds present in *A. ammoniophilus* and *S. gausapatum*. However, this requires that structures and physicochemical properties of the target compounds are well characterized before proceeding with downstream purification steps such as column chromatography.

As mentioned in the introduction, publicly available mass spectrometric databases are extensively and continuously updated [46]; yet only a few MAAs are included. Even if in one of our previous studies [38] several unambiguously identified MAAs were added, just a fraction of the more than 70 MAA structures known today is represented. Since the isolation of all these compounds would not only be extremely time-consuming but also require the collection and thorough processing of large amounts of biomass, we decided to pursue a different strategy.

In 2019, Nothias-Esposito et al. introduced a unique approach to analyze the profiles of premyrsinane and myrsinane esters in *Euphorbia cupanii* and *E. pithyusa* [49]. By leveraging the fact that a single *Euphorbia* species produces only a limited number of diterpene backbones esterified with characteristic short acyl substituents, they created a combinatorial database of theoretical premyrsinane and myrsinane derivatives using SmiLib software and applied it for “network annotation propagation” (NAP)-based annotation [60]. In simple terms, NAP propagates information from known compounds (spectral library matches) and/or from the top candidate structures of neighboring nodes

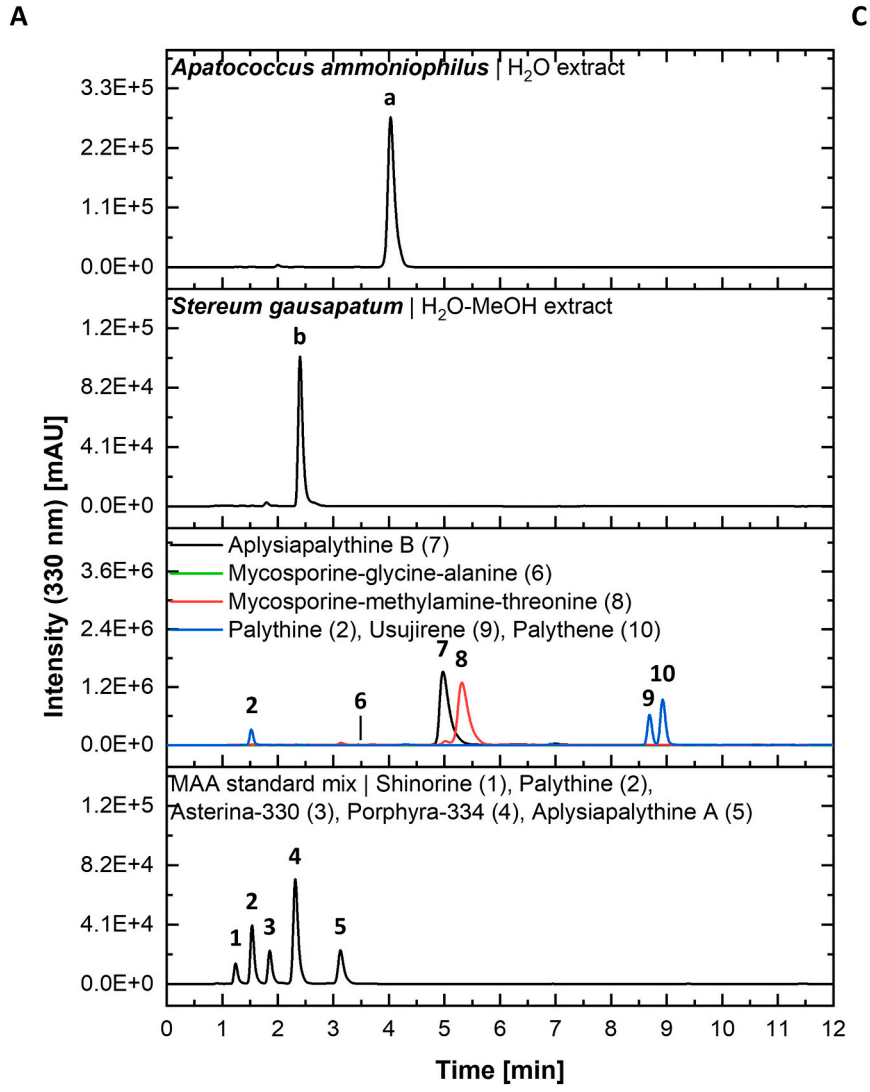

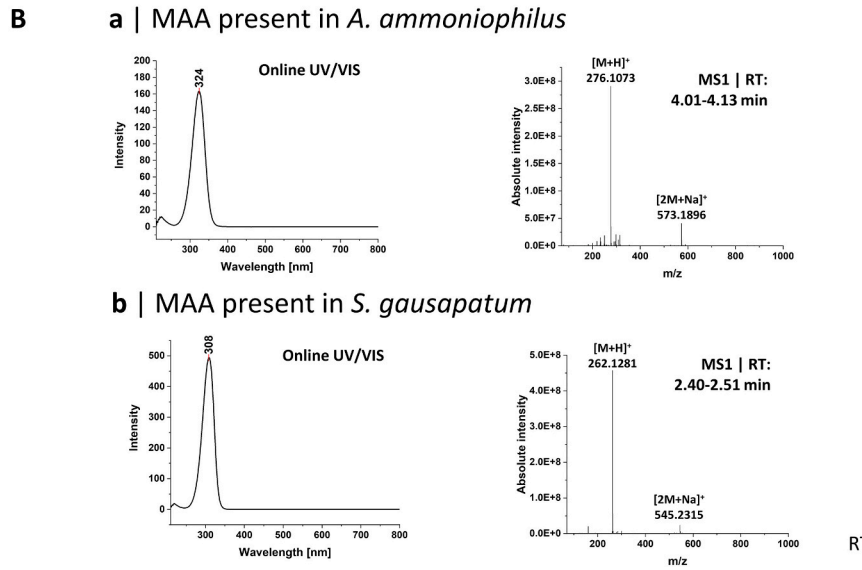

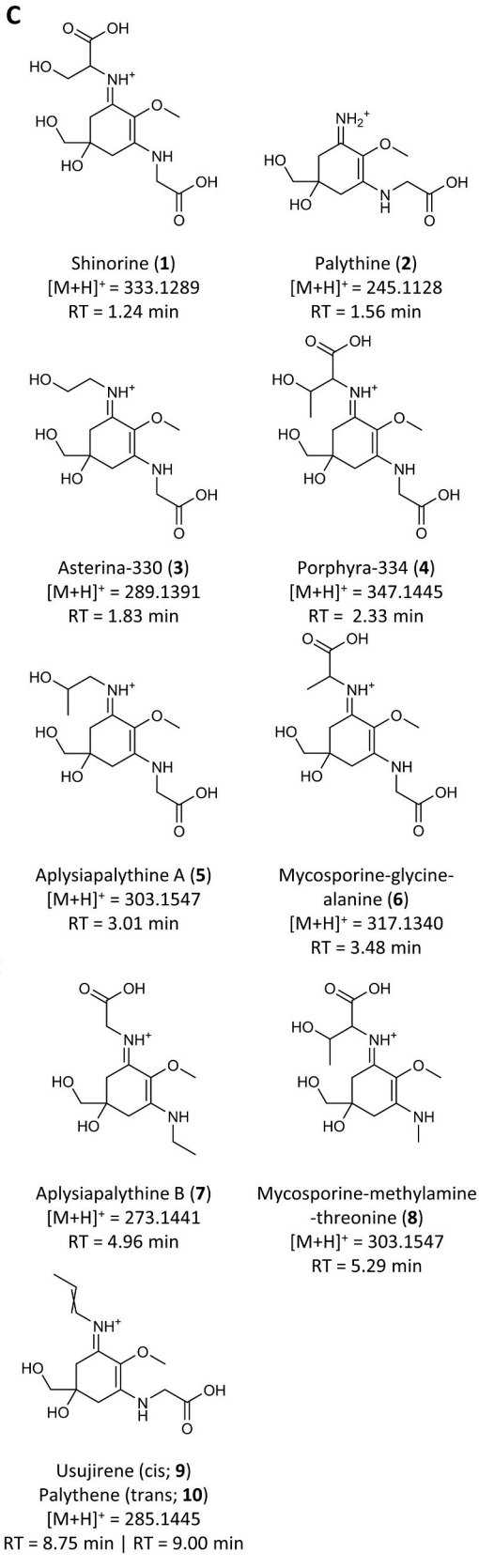

Fig. 2. A | UHPLC chromatograms of the H_2O extract of *A. ammoniophilus*, the aqueous methanolic extract of *S. gausapatum*, and several MAA reference compounds, recorded at a detection wavelength of 330 nm. B | Online UV/Vis spectra and high-resolution mass spectra (MS^1 level) of the putative MAAs detected in *A. ammoniophilus* (**a**) and *S. gausapatum* (**b**). C | Molecular structures, formulas, observed exact masses of the quasimolecular ions ($[M + H]^+$), and chromatographic retention times of the reference MAAs.

to unknowns within a molecular network. This approach enabled the identification of 123 premyrsinane or myrsinane esters, 74% of which were not found in any existing compound database. Similarly, Xe et al. (2023) employed a combinatorial database of pyrrolizidine alkaloids to annotate these metabolites in three traditional Chinese medicinal plants (*Arnebia euchroma*, *Senecio scandens*, and *Tussilago* sp.) [61].

The biosynthesis of MAAs remains an active field of research, with an increasing focus on heterologous expression in microorganisms like *Saccharomyces cerevisiae* [62] and *Escherichia coli* [63]. These approaches aim to advance the mechanistic understanding of MAA biosynthesis and to establish scalable production systems for compound isolation. In cyanobacteria, the MAA biosynthetic pathway is primarily linked to the pentose phosphate pathway, where sedoheptulose 7-phosphate is converted into 4-deoxygadusol through the action of 2-*epi*-5-*epi*-valiolone synthase (EEVS) and an *O*-methyltransferase. Subsequently, various amino acids can condense with the resulting core structure to form a diversity of MAAs. In addition to this route, biosynthesis via the shikimate pathway has also been described [64]. Interestingly, the Mahmud group demonstrated that certain vertebrates possess EEVS and a bifunctional enzyme capable of converting sedoheptulose 7-phosphate into gadusol [6].

Overall, MAAs are characterized by a limited number of core scaffolds that can be conjugated with different amino acids, leading to the observed structural diversity. This modular nature renders MAAs ideally suited for the creation of a combinatorial structure database. Following the concept introduced by Nothias-Esposito and colleagues, a set of input files for the software SmiLib was generated (Fig. 3). They included the core structures of cyclohexenone-, klebsormidin- (later referred to as algasporine-type), deoxyklebsormidin- (deoxyalgasporine-type), and cyclohexenimine-type MAAs, combined with a linker and a set of proteinogenic, non-proteinogenic, and decarboxylated amino acids. The resulting output, consisting of a list of SMILES codes representing the combinatorially generated MAAs, was subsequently converted using the OPENBABEL chemical file format converter. The converted list was exported, and complemented by literature-known MAAs, including those with hydrogen substitution such as palythine. In total, 4594 compounds with 1233 distinct molecular formulas were compiled and incorporated into SIRIUS to enable targeted annotation of putative MAAs.

3.4. Molecular networking-based annotation and isolation of MAAs

For the tentative identification of the two unknown compounds detected in *A. ammoniophilus* (a) and *S. gausapatum* (b), UHPLC-VWD-HRMS^2 data from the aqueous and aqueous methanolic extracts of both organisms were evaluated in combination with in-house available MAA references (Fig. 2A, Fig. 2C) using a molecular networking approach. In addition, a previously established UV-filter variable was applied to identify features (precursor ions with a defined retention time) exhibiting the characteristic absorption behavior of MAAs at 330 nm [38]. A chemotaxonomic classification of all detected features was obtained using CANOPUS within SIRIUS [56] and integrated as an additional information layer into the network visualization. The feature-based molecular network, generated through the GNPS workflow using the cosine similarity score, revealed that the feature corresponding to the putative MAA in *A. ammoniophilus* was located within a cluster comprising several nodes annotated as "Mycosporines and Mycosporine-like amino acids" (NPC class level) [65]. However, the feature (ID 1095) itself was classified as a "Phenylethylamine." The feature corresponding to the compound in *S. gausapatum* (ID 806) was part of a separate cluster but classified as a potential MAA at the class level. Both nodes, however, were not directly connected to the clusters containing the reference MAAs (Fig. 4A), which limited the confidence of their annotation. To refine clustering, a second molecular network was generated using the DreaMS algorithm [42], which employs an AI-based similarity scoring of MS^2 fragmentation spectra. In this network, both unknown (putative) MAAs were positioned within a subregion that also contained all reference MAAs (Fig. 4B), strengthening the likelihood that both compounds indeed represent MAAs.

SIRIUS yielded for compound **a** ($[M + H]^+$ *m/z* 276.1073) the

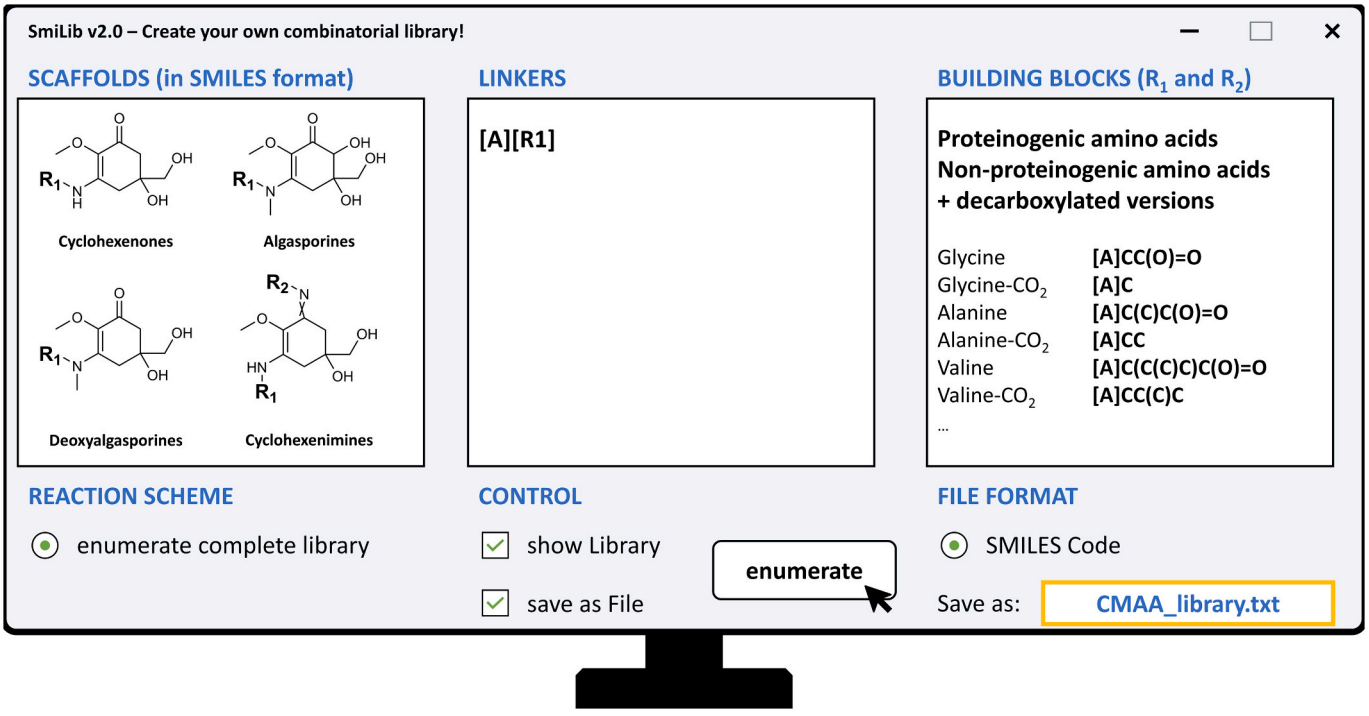

Fig. 3. Design concept for generating a combinatorial MAA database with SmiLib for targeted annotation of MAAs within SIRIUS. Cyclohexenone, algasporine (klebsormidin-type), deoxyalgasporine (deoxyklebsormidin-type), and cyclohexenimine cores (depicted with unspecified E/Z stereochemistry, as this cannot be inferred from MS data) were used as scaffolds, [A][R1] as linker, and a set of proteinogenic, non-proteinogenic, and decarboxylated amino acids for enumeration.

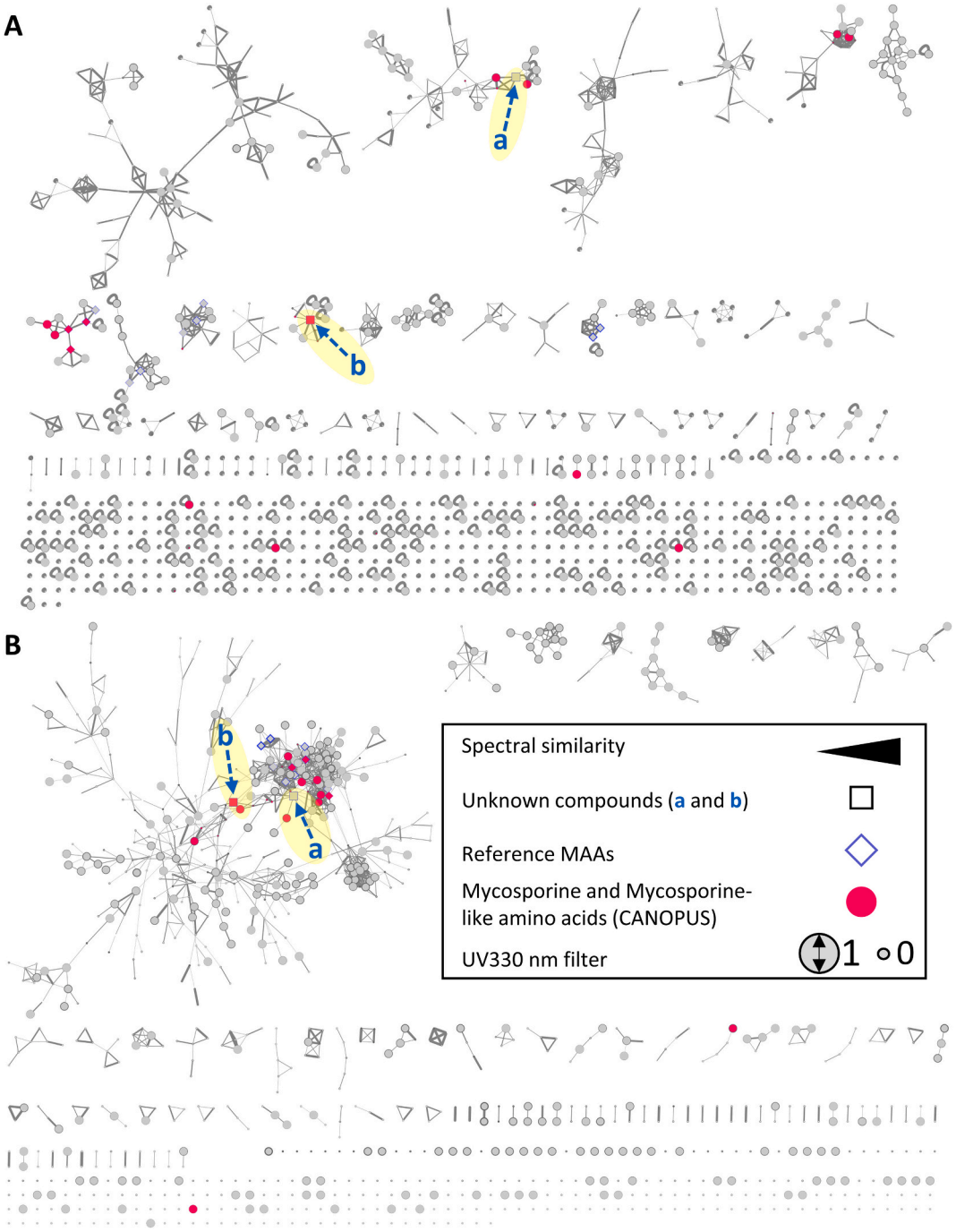

Fig. 4. Data visualized as feature-based molecular networks using different similarity scores (A = cosine score, B = DreaMS score).

molecular formula $C_{11}H_{17}NO_7$ with a median mass error of 0.151 ppm, and for compound **b** ($[M + H]^+$ *m/z* 262.1282) the molecular formula $C_{11}H_{19}NO_6$ with a median mass error of 1.205 ppm. To assess the output of SIRIUS in combination with the newly developed combinatorial MAA database, the annotation approach was first validated using reference compounds. Indeed, SIRIUS correctly assigned the structures of all reference MAAs, identifying shinorine, palythine, porphyra-334, and mycosporine-methylamine-threonine at rank 1, and aplysiapalythine A, aplysiapalythine B, mycosporine-glycine-alanine, usujirene, and palythene at rank 4. This indicates that while the workflow provides meaningful annotations, expert knowledge and the availability of reference compounds with well-defined retention times in (U)HPLC experiments remain indispensable for reliable compound annotation. Targeted annotation of the two unknown compounds using the combinatorial MAA database produced two hits for compound **a**: the previously suspected compound mycosporine-serine and a second structure featuring a gadusol core linked to glycine with an additional *N*-methyl substitution (CMAA_89, Fig. 5A). For compound **b**, the search indicated mycosporine-serinol and another related combinatorial MAA structure (Fig. 5A).

As *A. ammoniophilus* forms relatively thin mats, collecting sufficient biomaterial for isolation proved to be a tedious task, requiring manual removal with a brush. Ultimately, two compounds, **a** and gadusol, were obtained using a combination of liquid-liquid extraction, RP-MPLC, and RP-HPLC. However, the RP-HPLC fraction, initially presumed to contain a single (and HPLC-DAD-pure) compound, was later revealed to contain

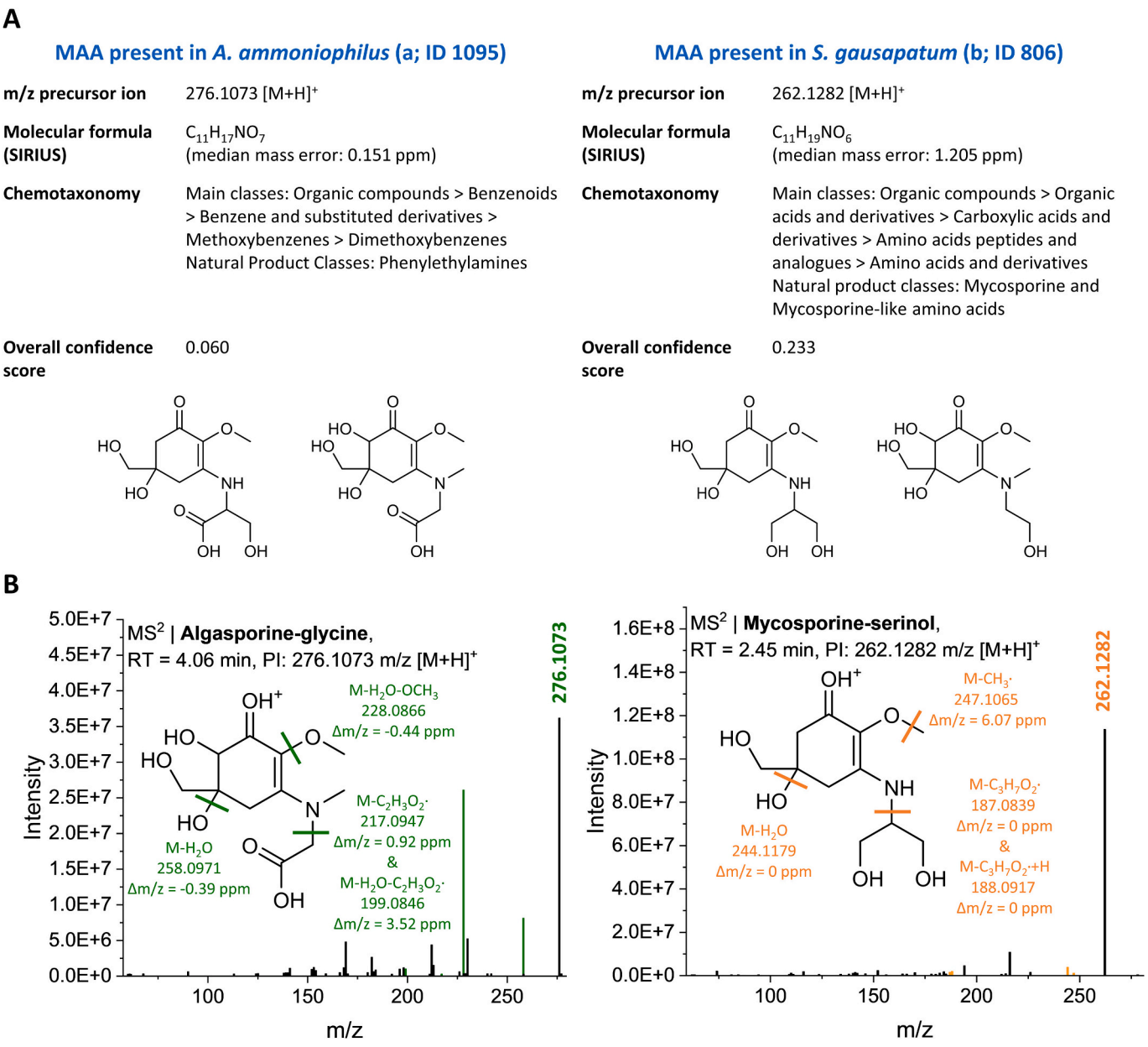

Fig. 5. A | Combinatorial MAA database annotation results for the two unknown MAAs present in *A. ammoniophilus* (**a**) and *S. gausapatum* (**b**), including feature ID, *m/z*, putative molecular formula, chemotaxonomy, and overall SIRIUS confidence score. B | MS^2 spectra of algasporine-glycine (**a**) and mycosporine-serinol (**b**) with key fragmentation reactions highlighted.

two distinct constituents by NMR spectroscopy. Their successful separation was possible only after applying semi-preparative hydrophilic interaction liquid chromatography (HILIC) (Fig. 6A). Previous attempts, including size-exclusion chromatography on Sephadex LH-20, had provided only partial separation. In the end, two compounds were obtained, eluting at 1.51 min (gadusol) and 4.06 min (compound **a**) in the UHPLC-VWD-$HRMS^2$ analysis.

For the feature corresponding to gadusol (ID 557), SIRIUS proposed the molecular formula $C_8H_{12}O_6$ (median mass error: −1.550 ppm), assigned it to the NPC compound class "Shikimic acids and derivatives", and identified gadusol as the top-ranked candidate (rank 1). The overall SIRIUS confidence score was 0.128, indicating rather weak support. NMR data (Table 1), however, provided conclusive structural evidence. The spectra exhibited a methoxy group (δ_C 58.1 ppm, δ_H 3.32 s) at carbon C-2 and a methylene group at position C-6 (δ_C 43.8 ppm, δ_H 2.40 d, 1.98 d). In addition, one hydroxymethine (δ_C 76.0 ppm, δ_H 3.81 s) and hydroxymethylene (δ_C 62.0 ppm, δ_H 3.44 d, 3.20 d) group were observed, showing key HMBC correlations to C-3 and C-5, respectively. The NMR data further indicated the presence of a vinylogous acid system extending from C-3 to C-1. The ^{13}C resonances at δ_C 178.2 (C-3, C═O), 131.9 (C-2, C-OCH_3), and 181.1 (C1, C-OH) were characteristic for an α,β-unsaturated carbonyl system (Fig. 6B). Overall, interpretation of the spectroscopic data confirmed the identity of the compound as gadusol. The MS^2 spectrum further supported this assignment, exhibiting characteristic fragmentations typical of mycosporines, including sequential losses of water and the methoxy group, yielding fragment ions at *m/z* 187.0598 (−1.60 ppm) and *m/z* 157.0493 (−1.27 ppm).

The 2D-NMR data of compound **a** (Table 1) indicated a cyclohexenone-type scaffold bearing a methoxy group (δ_C 59.1 ppm, δ_H 3.38 s) at carbon C-2 and a methylene group at C-6 (δ_C 34.5 ppm, δ_H 2.76 d, 2.19 d). Furthermore, one hydroxymethine (δ_C 76.9 ppm, δ_H 3.77 s) and one hydroxymethylene group (δ_C 62.1 ppm, δ_H 3.44 d, 3.20 d) were present, each showing diagnostic HMBC correlations to C-3 and C-5, respectively. The spectrum was consistent with a vinylogous amide

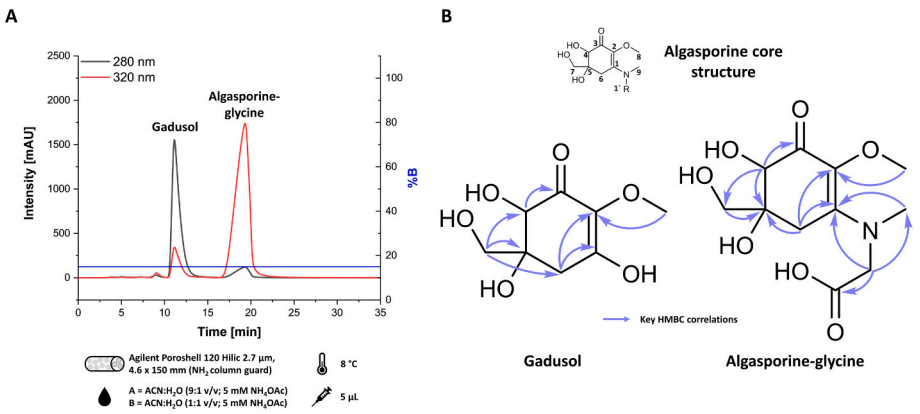

Fig. 6. A | Semi-preparative HILIC separation of the *A. ammoniophilus* fraction, which contained gadusol and algasporine-glycine. Important method parameters are listed below the figure. B | Molecular structures of the algasporine core, gadusol, and algasporine-glycine, with key $^{1}H—^{13}C$ HMBC correlations indicated by purple arrows. (For interpretation of the references to colour in this figure legend, the reader is referred to the web version of this article.)

Table 1
^{1}H (400.13 MHz) and ^{13}C (100.61 MHz) NMR data of mycosporine-serinol (compound **b** from *S. gausapatum*), gadusol, and algasporine-glycine (compound **a** from *A. ammoniophilus*). All spectra were recorded in DMSO-d_6. For ease of comparison, a uniform numbering scheme was applied to all compounds, assigning the lowest number to the *N*-substituent (side chain). * … exchangeable.

	Mycosporine-serinol			Gadusol			Algasporine-glycine		
Pos.	δ_C [ppm]	δ_H (*J* in Hz) [ppm]	HMBC	δ_C [ppm]	δ_H (*J* in Hz) [ppm]	HMBC	δ_C [ppm]	δ_H (*J* in Hz) [ppm]	HMBC
1	152.2			181.1			153.3		
2	130.0			131.9			129.9		
3	184.8			178.2			187.9		
4	45.2	2.43 (d, *J* = 16.3 Hz, 1H) 2.02 (d, *J* = 16.3 Hz, 1H)	3, 5, 6 2, 3, 5, 6	76.0	3.81 (s, 1H)	3, 5, 7	76.9	3.77 (s, 1H)	3, 5, 6, 7
5	71.7			74.7			75.1		
6	33.5	2.75 (d, *J* = 16.9 Hz, 1H) 2.40 (d, *J* = 16.9 Hz, 1H)	1, 2, 3 (weak), 4, 5 1, 2, 4, 5, 8,	43.8	1.98 (d, *J* = 16.0, 1H) 2.40 (d, *J* = 16.0, 1H)	1, 5, 7 1, 2, 5, 7	34.5	2.19 (d, *J* = 15.8, 1H) 2.76 (d, *J* = 16.0, 1H)	1, 2, 5, 7 1, 2, 5, 7
7	68.3	3.21 (s, 2H)	1 (weak), 3 (weak), 4, 5, 6,	62.0	3.20 (d, *J* = 11.0, 1H) 3.44 (d, *J* = 11.0, 1H)	4, 6 5, 6	62.1	3.33 (q, *J* = 11.8, 2H)	5, 6
8	58.2	3.46 (s, 3H)	2	58.1	3.32 (s, 3H)	2	59.1	3.38 (s, 3H)	2
9							41.4	3.06 (s, 3H)	1, 1’
N		N*H*: 6.00 (d, *J* = 9.0 Hz, 1H)	2, 6, 1′, 2′, 3’						
1′	55.6	3.42 (part of a large multiplet, 1H)					58.4	3.66 (d, *J* = 17.1, 1H) 3.77 (d, *J* = 17.1, 1H)	1, 9, 2′ 1, 9, 2’
2′	61.1*	3.45 (part of a large multiplet, 2H)	No unambiguous assignment possible				171.0		
3′	60.9*	3.45 (part of a large multiplet, 2H)	No unambiguous assignment possible						

system extending from C-3 (δ_C 187.9 ppm, C═O) through C-2 (δ_C 129.9 ppm, C-OCH_3) to C-1 (δ_C 153.3 ppm). In addition, an *N*-methyl group (δ_C 41.4 ppm, δ_H 3.06 s) exhibited cross-peaks to C-1 and C-1′, confirming substitution at the nitrogen atom (Fig. 6B).

The amino acid substituent was identified as glycine, based on the presence of a single methylene group (δ_C 58.4 ppm, δ_H 3.66 d, 3.77 d) that coupled with both the *N*-methyl signal and the carbonyl carbon of the carboxyl moiety (δ_C 171.0 ppm, COOH). Tandem MS experiments supported this structural interpretation, showing fragmentation pathways typical for MAAs, including sequential losses of water, a methoxy group, and the carboxymethylene part of the glycine residue (Fig. 5B).

Taken together, these findings, along with the SIRIUS-based annotation using the combinatorial MAA database, ruled out the initially suggested identity as mycosporine-serine, instead a new MAA was found. Compound **a** from *A. ammoniophilus* was thus identified as *N*-(4,5-dihydroxy-5-(hydroxymethyl)-2-methoxy-3-oxocyclohex-1-en-1-yl)-*N*-methylglycine, for which the trivial name algasporine-glycine is proposed.

This trivial name is taxonomically inspired and intended to reflect key structural characteristics of the compound. It is proposed as part of a provisional nomenclature framework rather than as a new classification of MAAs. The first MAAs were discovered in fungi, which led to the term mycosporine [66]. In recent years, however, several structurally related analogues have been reported from algal sources, such as *Klebsormidium crenulatum* (klebsormidin A and B) [2] and members of the Prasiolaceae family [3,67]. These compounds, with the exception of prasiolin, share a gadusol-type chromophore and an *N*-methyl substituent, distinguishing them from the classical mycosporines. Additionally, they exhibit

characteristic UV absorption spectra with a maximum at 320 or 324 nm. Although the current taxonomic coverage of terrestrial algae, cyanobacteria, and fungi remains limited, these observations suggest the existence of a distinct subgroup of related MAAs. To facilitate structurally informative naming of present and future representatives, a provisional naming convention based on the term algasporine is proposed. Within this framework, klebsormidin A could be designated as algasporine-serine-glucopyranoside, klebsormidin B as algasporine-serine, and the compound reported by Rainer et al. as algasporine-asparagine [67]. Likewise, prasiolin could be referred to as noralgasporine-glutamic acid, with the prefix "nor-" indicating the absence of the *N*-methyl group while still featuring the gadusol core structure. Hence, the newly isolated compound from *A. ammoniophilus* was named algasporine-glycine (Table S2). Importantly, this proposal is not intended to replace the established distinction between cyclohexenone- and cyclohexenimine-type MAAs, nor the nomenclature of MAAs possessing the classical deoxygadusol core and lacking *N*-methyl substitution, which may retain their established names. Rather, it provides a complementary and structurally informative naming framework, particularly regarding the core structure (i.e., a gadusol core with *N*-methyl substitution) whose broader applicability will need to be evaluated as additional MAAs are characterized. It can also be readily extended to cyclohexenimine-type MAAs by appending the second amino acid residue to the compound name. For example, a (theoretical) cyclohexenimine-type MAA possessing a gadusol core, an *N*-methylglycine substituent, and an alanine residue could be designated algasporine-glycine-alanine.

Compound **b** was isolated from the dried and milled fruiting bodies of *S. gausapatum* collected in 2023 in Eppan (South Tyrol). After defatting, targeted extraction of the putative MAA was performed using methanol and aqueous methanol as solvents. Both polar extracts were subsequently partitioned between water and *n*-butanol to remove carbohydrate-like matrix components. The resulting fraction was further purified by RP-MPLC, followed by reversed-phase semi-preparative HPLC. In the UHPLC-VWD-HRMS^2 experiments, the compound eluted at approximately 2.45 min and showed a proton adduct at *m/z* 262.1282, corresponding to the molecular formula $C_{11}H_{19}NO_6$ with a low mass error, indicating a high level of confidence. The NMR spectra (see supplementary material) confirmed the presence of a cyclohexenone-type MAA scaffold. Characteristic signals (Table 1) for ring-associated methylene groups were observed at carbons C-4 and C-6 (δ_C 45.2, δ_H 2.43 d, 2.02 d; δ_C 33.5, δ_H 2.75 d, 2.40 d), along with a hydroxymethylene group at C-7 (δ_C 68.3, δ_H 3.21 s). HMBC correlations from the *N*—H proton (δ_H 6.00 d) to carbons C-2 (δ_C 130.0) and C-6 (δ_C 33.5) confirmed substitution at carbon C-1.

In the ^{1}H NMR spectrum, the region between 3.70 and 3.35 ppm contained signals corresponding to a methoxy group (δ_C 58.2, δ_H 3.46 s) attached to carbon C-2, as well as to two methylene and one methine proton from the 1,3-dihydroxypropan-2-yl (serinol) side chain. Although some multiplicities and HMBC correlations within this region were difficult to assign unambiguously, the calculated molecular formula, the annotation obtained via SIRIUS, and the overall NMR data strongly support identification of the compound as mycosporine-serinol. The MS^2 spectrum (Fig. 5B) further corroborated this structural proposal, exhibiting characteristic MAA-specific fragmentation patterns [68,69], including the loss of a CH_3 radical (methoxy group), the loss of water, and, in this particular case, fragmentation corresponding to cleavage of the 1,3-dihydroxypropan-2-yl side chain.

3.5. MAA profiling

A total of 31 *A. ammoniophilus* samples collected in Denmark were examined in biological duplicates for their gadusol and algasporine-glycine content using HPLC-DAD. Overall, gadusol concentrations ranged from zero (below the limit of detection) to 0.337 mg g^{-1} dry weight (DW), while algasporine-glycine levels varied between 0.032 and 2.311 mg g^{-1} DW. The gadusol-richest samples originated from Jutland (Thy, Thagårds Plantage) with 0.337 ± 0.041 mg g^{-1} DW, and from another site near Esbjerg (Jutland, 14 km NW of Esbjerg) collected from *Pinus nigra* bark, showing 0.296 ± 0.020 mg g^{-1} DW. The highest algasporine-glycine concentrations were found in one sample from Jutland (Grene Sande) growing on *Prunus padus* with 2.311 ± 0.202 mg g^{-1} DW, and another from Jutland (Baldersbæk Plantage) collected from *Pinus* sp. bark and twigs with 2.043 ± 0.052 mg g^{-1} DW. Overall, both compounds showed considerable quantitative variation among the samples. In a previous study, Hotter et al. (2018) reported in numerous members of the terrestrial *Prasiola* clade prasiolin concentrations between 10 μg g^{-1} DW (*Stichococcus bacillaris*) and 58 mg g^{-1} DW (*Prasiolopsis ramosa*), indicating also a very high species-specific and sample variability [70]. The high algasporine-glycine variability can be explained by constitutive traits, environmental factors (e.g., season, exposition to the sun, nitrogen availability) and/or spatial position in a biofilm. In addition, although most field samples were dominated by *A. ammoniophilus*, co-occurring algal taxa cannot be excluded, which would affect the concentration.

In the HPLC-DAD experiments, several additional peaks with absorption properties characteristic of MAAs (λ_{max} = 310–330 nm) were noticed aside from the two quantified compounds (Fig. 7A). Consequently, we investigated the overall MAA profile in the samples using our established UHPLC-VWD-HRMS^2 workflow. The resulting data were processed and subjected to feature-based molecular networking (FBMN) on the GNPS2 platform for visualization and evaluation. The generated network comprised 727 nodes connected by 295 edges, forming 30 clusters with three or more nodes, while 420 nodes remained as singletons (Fig. 7A).

SIRIUS-based compound class annotation revealed that the dominant classes (NPC class level) were "Amino acids" (144 features, 24.2%), "Amino sugars" (34, 5.7%), "Cyanogenic glycosides" (30, 5.0%), "Dipeptides" (29, 4.9%), and "Imidazole alkaloids" (28, 4.7%). Eleven features (1.8%) were putatively identified as "Mycosporine and Mycosporine-like amino acids (MAAs)". A complementary search using the combinatorial MAA database resulted in 34 potential hits. Application of the UV-based filter highlighted 148 features (20.4% of all nodes) with the expected absorption properties. When all UHPLC-VWD chromatograms were overlaid, seven distinct UV-absorbing peaks consistent with putative MAAs became apparent, and their corresponding features were distributed among four separate molecular clusters in the FBMN.

Cluster I, comprising 22 nodes and connected by 52 edges, contained four nodes annotated at the class level as MAAs (Fig. 7B). This cluster included the main MAA detected in *A. ammoniophilus*, algasporine-glycine (#1, ID 520), along with its sodium adduct. Another feature within the same cluster (#2, ID 591; RT = 6.01 min; *m/z* 262.1302) was connected to the algasporine-glycine node and tentatively identified as an algasporine core substituted with a hydroxyethyl group based on its combinatorial MAA database match. Ion identity molecular networking (IIMN) [41] revealed two additional features corresponding to the sodium and potassium adducts of #2. A further, slightly more apolar feature (#3, ID 611; RT = 6.63 min; *m/z* 232.1192) was also present in this cluster and putatively annotated as the decarboxylated derivative of algasporine-glycine. Moreover, gadusol (#4, ID 313) and its $[M\text{-}H_2O + H]^+$ adduct were also located within cluster I.

Cluster II contained six nodes connected by seven edges, two of which were putatively annotated as MAAs (Fig. 7B). Among them, one feature (#5, ID 490; RT = 3.23 min; *m/z* 465.2110) with corresponding sodium and potassium adducts was annotated as mycosporine-glutaminol-*O*-glucoside. This compound was initially found in terrestrial microcolonial ascomycetes such as *Sarcinomyces petricola* and *Coniosporium* spp., as well as in *Botryosphaeria*-like fungi [71,72]. It was later identified by Sommaruga et al. (2004) in the basidiomycetous yeasts *Rhodotorula minuta* and *R. slooffiae* [73]. More recently, Martins-Silva and colleagues demonstrated that the mycosporine-glutaminol-*O*-glucoside production is enhanced by UVR in *Naganishia friedmannii*. They linked it to the UV-dependent induction of a biosynthetic gene

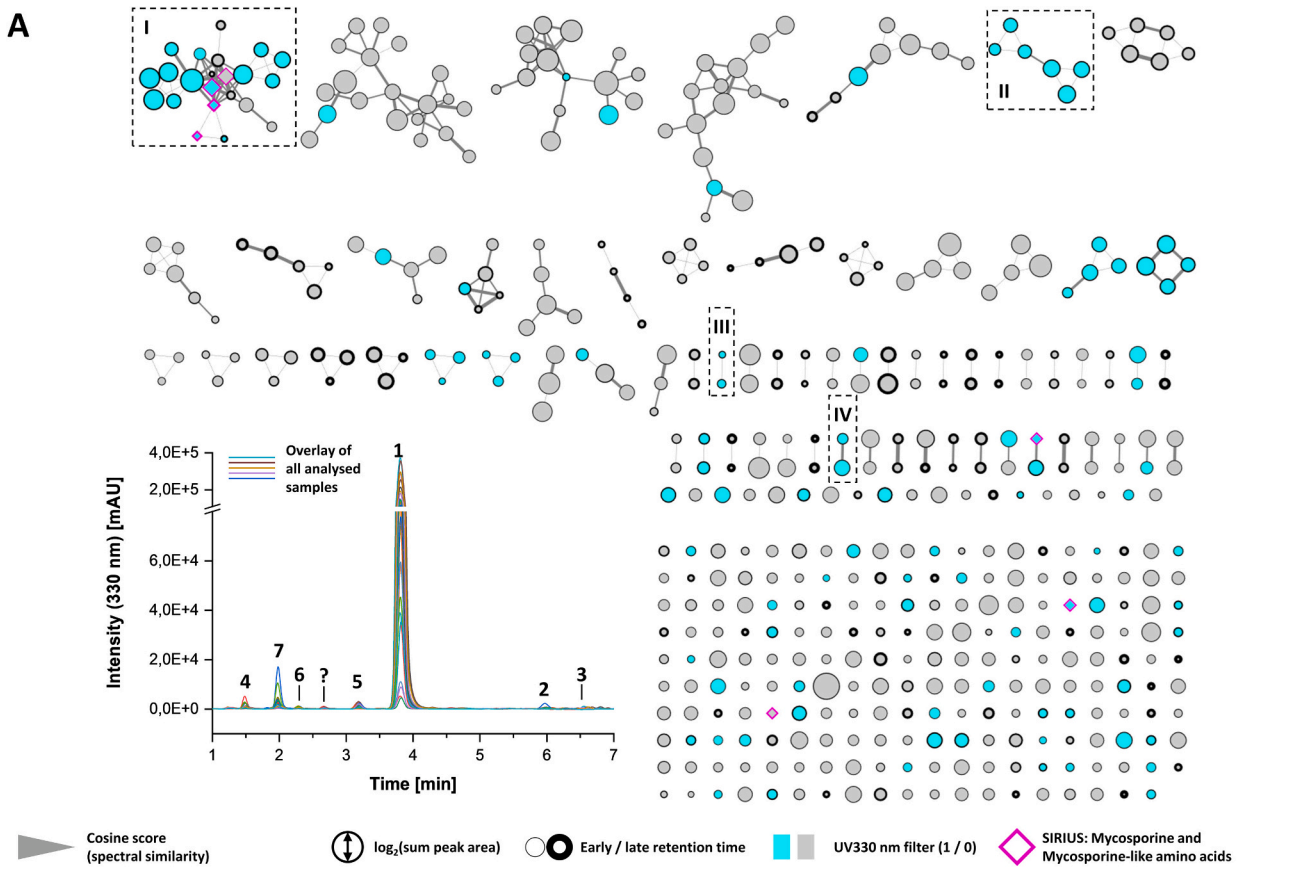

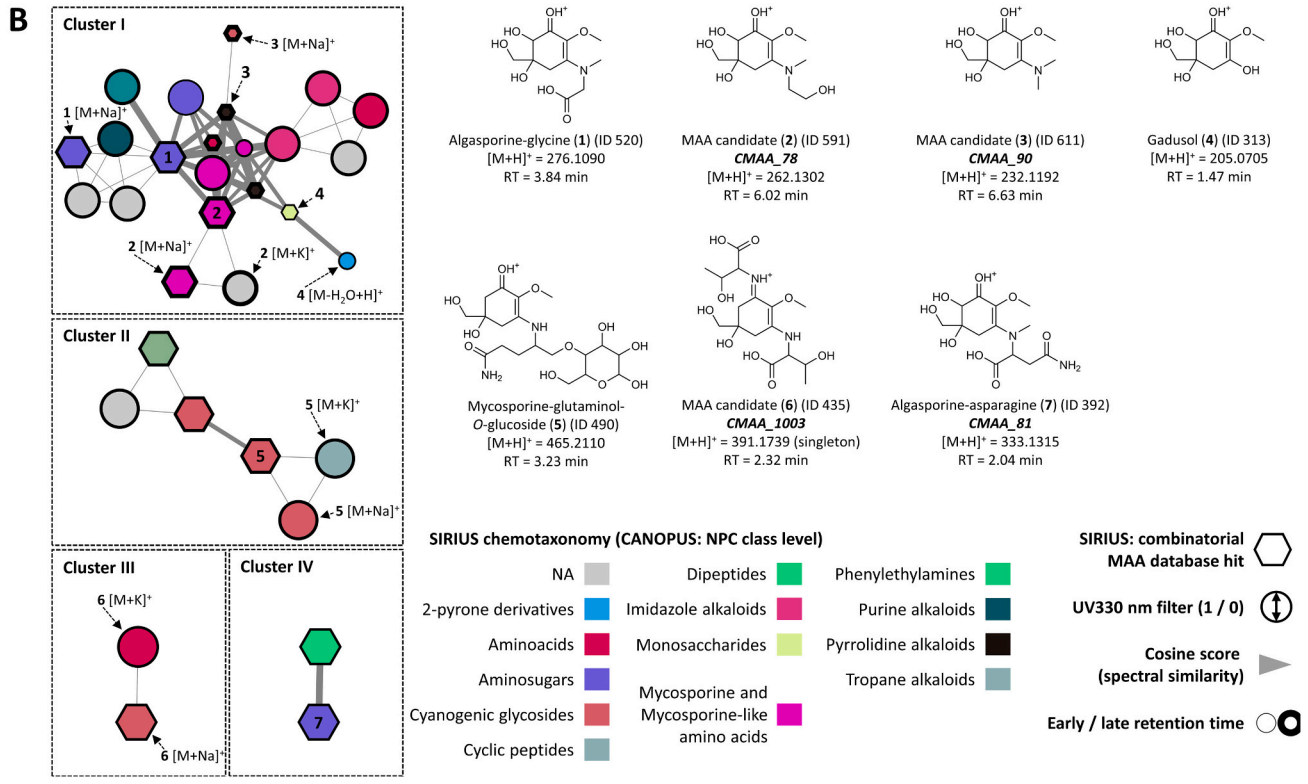

(caption on next page)

Fig. 7. A | Feature-based molecular network generated from 31 extracts of different *A. ammoniophilus* samples, together with an overlay of their HPLC chromatograms recorded at 330 nm (some parts of the network are obscured due to overlay). Clusters potentially containing MAAs are highlighted by black dotted-line boxes and labeled I-IV. Nodes annotated as MAAs via SIRIUS are displayed as pink-bordered diamonds. Node size reflects feature abundance (log_2-transformed total peak area across all extracts). UV absorption characteristics are colour-coded: nodes filled in cyan represent features co-eluting with a 330 nm-absorbing peak (UV_{330} filter = 1), whereas grey nodes indicate features without such behavior (UV_{330} filter = 0). Node border thickness corresponds to retention time, increasing with later elution. The thickness of the connecting edges indicates spectral similarity between two nodes. B | Detailed view of MAA-containing clusters. Nodes matching entries from the combinatorial MAA database within SIRIUS are shown as octagons. Fill colors denote chemotaxonomic classifications at the NPC class level obtained via CANOPUS. Putative annotation results, including molecular structures, observed *m/z* values, trivial names, and retention times, are shown on the right. Node size again represents the UV filter variable, with larger nodes indicating absorption at 330 nm. Numbering of annotated compounds corresponds to the labels on the right. (For interpretation of the references to colour in this figure legend, the reader is referred to the web version of this article.)

cluster involved in the mycosporine biosynthesis pathway [74].

Within cluster III, two features were assigned as sodium and potassium adducts of a compound whose protonated form did not cluster and remained a singleton in the network (#6, ID 435; RT = 2.32 min; *m/z* 391.1739) (Fig. 7B). These features were putatively annotated as a deoxygadusol derivative substituted with two threonine residues (CMAA_1003).

Cluster IV, also containing two nodes classified as MAAs, included one feature (#7, ID 392) tentatively identified as algasporine-asparagine (Fig. 7B). This compound was previously reported by Rainer et al. as a secondary metabolite of a member from the Prasiolaceae family; however, the exact algal species was not specified [67].

One additional minor UV-absorbing peak, eluting between peaks #6 and #5, could not be annotated. With the exception of algasporine-glycine (#1) and gadusol (#4), all other compounds remain putatively identified; thus, their unambiguous structural confirmation will require isolation and NMR-based characterization. Nevertheless, the workflow successfully provided structural suggestions for seven out of eight UV-absorbing peaks, most of which would represent novel or algasporine-type MAAs. Notably, several of these tentatively identified structures are located in the same molecular cluster as the verified reference compounds, providing additional confidence in their annotation. These findings are particularly encouraging, as preliminary results indicate that biotechnological culturing of the investigated algal species is feasible (unpublished results), enabling the future isolation and structural elucidation of low-abundance MAAs.

3.6. Antioxidative activity and cytotoxicity of the isolated compounds

One of the key mechanisms underlying UV-A- and UV-B-induced photodamage is the generation of ROS and the resulting oxidative stress. Excessive ROS production can overwhelm cellular antioxidant defense systems and lead to oxidative damage of key biomolecules, including lipids, proteins, and nucleic acids [75]. To explore the potential of MAAs to counteract ROS-mediated effects in human skin cells, HaCaT keratinocytes were pre-treated with the isolated MAAs mycosporine-serinol and algasporine-glycine prior to the induction of intracellular ROS formation using the chemical radical generator AAPH. Antioxidative activity was assessed by measuring DCF fluorescence [58]. In parallel, potential cytotoxic effects following short-term exposure to MAAs were evaluated. Treatment with AAPH resulted in a more than 15-fold increase in intracellular ROS levels. Mycosporine-serinol did not exhibit a protective effect against ROS formation, whereas the newly discovered MAA algasporine-glycine caused a statistically significant reduction in ROS levels (Fig. 8A). Importantly, neither compound showed cytotoxic effects at concentrations of up to 1 mM, demonstrating excellent cellular tolerability (Fig. 8B). These results suggest that mycosporine-serinol and algasporine-glycine are well tolerated by human keratinocytes and support the further evaluation of algasporine-glycine as potential UV-protective compound. Additional studies will be required to assess the full range of antioxidative capacities of MAAs under UV-induced oxidative stress conditions, which more closely reflect the physiological context of solar exposure.

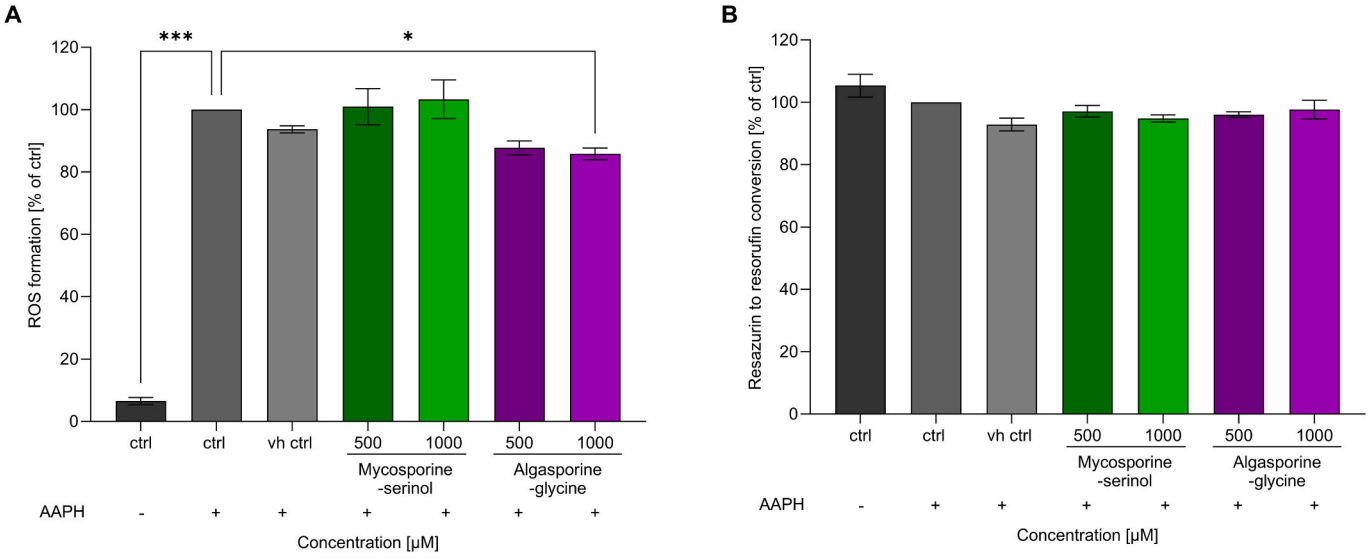

Fig. 8. Evaluation of antioxidative activity and cellular tolerability of selected MAAs in HaCaT keratinocytes. A | Intracellular reactive oxygen species (ROS) levels were measured using a 2′,7′-dichlorodihydrofluorescein diacetate (DCFH-DA)-based assay following induction with a water-soluble free radical generator (2,2′-azobis (2-amidinopropane) dihydrochloride (AAPH)). Treatment with algasporine-glycine resulted in a minor but significant reduction of intracellular ROS levels, whereas mycosporine-serinol showed no effects under the tested conditions. B | Cell viability at 2 h post-treatment was assessed using a resazurin-based metabolic activity assay. No cytotoxic effects were observed for either compound compared to the control. Data are presented as mean ± SEM of four independent experiments performed in triplicates. Statistical significance is indicated as $p < 0.05$ (*) and $p < 0.001$ (**).

4. Conclusion

In this study, we established a rational combinatorial MAA database based on the structural variability of known core scaffolds and their possible substituents, and integrated it into the bioinformatic software SIRIUS. Coupled with UHPLC-VWD-HRMS^2 screening and feature-based molecular networking, this strategy enabled the putative identification of mycosporine-serinol and the previously undescribed algasporine-glycine in *S. gausapatum* and *A. ammoniophilus*, respectively. The latter compound was isolated and structurally identified as a novel natural product. The presented workflow, which combines chromatographic separation, molecular networking, and combinatorial database-assisted annotation, provides a powerful and transferable strategy for the pre-identification of natural products that follow a scaffold-substituent relationship and constitutes a valuable contribution towards more efficient and reliable MAA annotation in complex extracts.

From a biological perspective, our findings add to current knowledge of photoprotective strategies in aeroterrestrial microalgae. The observed quantitative and qualitative variation in gadusol, algasporine-glycine, and additional putative algasporine-type MAAs among Danish field samples indicates that MAA composition can differ between populations and sites, and hence suggests that *A. ammoniophilus* may provide a useful system for future studies on photoprotection, stress physiology, and nitrogen pollution in terrestrial environments. Another interesting aspect is the missing pyrenoid in *A. ammoniophilus* [1], which in other algal groups strongly enhances the activity of the CO_2-fixing enzyme RubisCO by supplying it with concentrated carbon. We therefore speculate that the lack of this important organelle might be compensated by the presence of atypical MAAs, which could serve as an alternative organic carbon source for RubisCO or contribute to cellular C/N homeostasis.

Cellular assays further indicate that the newly discovered algasporine-glycine exerts measurable intracellular ROS-scavenging activity in human HaCaT keratinocytes without detectable short-term cytotoxicity at concentrations up to 1 mM, whereas mycosporine-serinol is well tolerated but inactive under the tested conditions. Together with previous reports on the photoprotective, antioxidant, and wound-healing properties of MAAs, these data highlight *A. ammoniophilus* as a promising natural source of structurally diverse UV-absorbing metabolites with potential applications in dermatological and cosmeceutical formulations.

Several future investigations are possible to further refine and expand the findings presented here. If cultivation of *A. ammoniophilus* can be established and managed reliably, this would substantially improve biomass availability for detailed activity studies of algasporine-glycine and other low-abundance MAAs, including assays under UV-induced stress and in advanced, physiologically relevant skin models. Furthermore, to better assess their potential for cosmetic applications, additional studies would be required to evaluate properties such as photostability, thermal stability, and long-term safety and tolerability. In parallel, the many tentatively annotated algasporine-type and gadusol-derived metabolites detected in *A. ammoniophilus* require targeted isolation and full spectroscopic characterization, which would confirm MAA diversity and support more robust chemotaxonomic comparisons within Trebouxiophyceae. Integrating metabolomic profiles with genomic and transcriptomic data from *A. ammoniophilus* and related taxa may enable the identification of putative MAA biosynthetic gene clusters, providing a basis for functional studies and, ultimately, heterologous expression or metabolic engineering approaches. Finally, expanding MAA profiling to field samples systematically collected along gradients of nitrogen deposition, irradiation, and microclimate could help clarify how environmental factors shape MAA composition and lead to a more nuanced understanding of the ecological role of this currently spreading aerophytic alga.

CRediT authorship contribution statement

Fabian Hammerle: Writing – review & editing, Writing – original draft, Visualization, Methodology, Investigation, Formal analysis, Data curation, Conceptualization. **Ulrik Søchting:** Writing – review & editing, Investigation. **Armin Oberosler:** Writing – review & editing, Writing – original draft, Investigation. **Cornelia A. Karg:** Writing – review & editing, Writing – original draft, Visualization, Investigation. **Michael J. Zwerger:** Investigation, Conceptualization. **Christina Stöckholzer:** Investigation. **Stefan Schwaiger:** Writing – review & editing, Formal analysis. **Ursula Peintner:** Investigation. **Johanna M. Gostner:** Writing – review & editing, Funding acquisition. **Ulf Karsten:** Writing – review & editing, Funding acquisition, Conceptualization. **Markus Ganzera:** Writing – review & editing, Supervision, Project administration, Funding acquisition, Conceptualization.

Declaration of Generative AI and AI-assisted technologies in the writing process

During the preparation of this work ChatGPT and Perplexity Pro were employed in order to improve the readability and language of the manuscript. After using these tools, the authors carefully reviewed and adapted the content as needed and take full responsibility for the published article.

Funding

The authors declare financial support was received for the research and publication of this article. This research was funded in part by the Austrian Science Fund (FWF) [grant DOI 10.55776/I6122] and by the German Research Foundation (DFG) [grant number KA899/45-1] (FWF-DFG DACH project UVision). For open access purposes, the author has applied a CC BY public copyright license to any author accepted manuscript version arising from this submission.

Declaration of competing interest

The authors declare that they have no known competing financial interests or personal relationships that could have influenced the work reported in this study.

Appendix A. Supplementary data

- Detailed experimental procedures for sample preparation, extraction, and isolation of MAAs. In addition, the MS data preprocessing, the generation of feature-based molecular networks using different clustering algorithms, the preparation of MAA filter variables, and a description of annotation levels are provided.
- Complete annotation results of the *A. ammoniophilus* screening study, organized by molecular network clusters.
- Thin-layer chromatography (TLC) figures of the generated fractions.
- 1D- and 2D-NMR spectra of gadusol, algasporine-glycine, and mycosporine-serinol, along with remarks on the proposed nomenclature for the “algasporines”.
- Quantification results (HPLC-DAD) for gadusol and algasporine-glycine in *A. ammoniophilus* samples collected across Denmark.

Supplementary data to this article can be found online at https://doi.org/10.1016/j.algal.2026.104937.

Data availability

To adhere to FAIR practices in computational metabolomics [76], all necessary data to replicate the presented results as well as the combinatorial MAA database are available via zenodo: https://zenodo.org/records/18478940.

References

[1] U. Søchting, T. Friedl, Ø. Moestrup, F. Grewe, Y. Sun, Y.T. Çakır, et al., Mass development of a filamentous and likely nitrophilous aerophytic green alga on tree bark: *Apatococcus ammoniophilus* sp. nov. (Chlorophyta, Trebouxiophyceae), Front. Microbiol. 16–2025 (2025), https://doi.org/10.3389/fmicb.2025.1633308.

[2] A. Hartmann, K. Glaser, A. Holzinger, M. Ganzera, U. Karsten, Klebsormidin a and B, two new UV-sunscreen compounds in green microalgal *Interfilum* and *Klebsormidium* species (Streptophyta) from terrestrial habitats, Front. Microbiol. 11–2020 (2020), https://doi.org/10.3389/fmicb.2020.00499.

[3] A. Hartmann, A. Holzinger, M. Ganzera, U. Karsten, Prasiolin, a new UV-sunscreen compound in the terrestrial green macroalga Prasiola calophylla (Carmichael ex Greville) Kützing (Trebouxiophyceae, Chlorophyta), Planta 243 (1) (2016) 161–169, https://doi.org/10.1007/s00425-015-2396-z.

[4] V. Geraldes, E. Pinto, Mycosporine-like amino acids (MAAs): biology, chemistry and identification features, Pharmaceuticals 14 (1) (2021) 63, https://doi.org/10.3390/ph14010063.

[5] S. Asamizu, P. Xie, C.J. Brumsted, P.M. Flatt, T. Mahmud, Evolutionary divergence of sedoheptulose 7-phosphate cyclases leads to several distinct cyclic products, J. Am. Chem. Soc. 134 (29) (2012) 12219–12229, https://doi.org/10.1021/ja3041866.

[6] A.R. Osborn, K.H. Almabruk, G. Holzwarth, S. Asamizu, J. LaDu, K.M. Kean, et al., De novo synthesis of a sunscreen compound in vertebrates, eLife 4 (2015) e05919, https://doi.org/10.7554/eLife.05919.

[7] M. Chen, Y. Jiang, Y. Ding, Recent progress in unraveling the biosynthesis of natural sunscreens mycosporine-like amino acids, J. Ind. Microbiol. Biotechnol. 50 (1) (2023), https://doi.org/10.1093/jimb/kuad038.

[8] J.M. Shick, W.C. Dunlap, Mycosporine-like amino acids and related gadusols: biosynthesis, acumulation, and UV-protective functions in aquatic organisms, Annu. Rev. Physiol. 64 (2002) 223–262, https://doi.org/10.1146/annurev.physiol.64.081501.155802.

[9] J. Bonin, F.J. Hammerle, M. Ganzera, U. Krumme, U. Karsten, UV-absorbing mycosporine-like amino acids in the eyes of temperate marine and freshwater fish species, Front. Mar. Sci. 11–2024 (2024), https://doi.org/10.3389/fmars.2024.1426861.

[10] F.J. Hammerle, R. Schöpf, C.A. Karg, U. Krumme, J.M. Gostner, U. Karsten, et al., Photoprotective mycosporine-like amino acids in different organs of Baltic flatfish species revealed by targeted and untargeted metabolomics analyses, Front. Mar. Sci. 12–2025 (2025), https://doi.org/10.3389/fmars.2025.1688685.

[11] F. Chioccara, A. Delia Gala, M. De Rosa, E. Novellino, G. Prota, Mycosporine aminoacids and related compounds from the eggs of fishes, Bull. Soc. Chim. Belg. 89 (12) (1980) 1101–1106, https://doi.org/10.1002/bscb.19800891212.

[12] W.C. Dunlap, D.M. Williams, B.E. Chalker, A.T. Banaszak, Biochemical photoadaptation in vision: U.V.-absorbing pigments in fish eye tissues, Comp. Biochem. Physiol., Part B:Comp. Biochem. 93 (3) (1989) 601–607, https://doi.org/10.1016/0305-0491(89)90383-0.

[13] D.S. Mason, F. Schafer, J.M. Shick, W.C. Dunlap, Ultraviolet radiation-absorbing mycosporine-like amino acids (MAAs) are acquired from their diet by medaka fish (*Oryzias latipes*) but not by SKH-1 hairless mice, Comp. Biochem. Physiol., Part A: Mol. Integr. Physiol. 120 (4) (1998) 587–598, https://doi.org/10.1016/S1095-6433(98)10069-7.

[14] U.E. Siebeck, N.J. Marshall, Ocular media transmission of coral reef fish — can coral reef fish see ultraviolet light? Vision Res. 41 (2) (2001) 133–149, https://doi.org/10.1016/S0042-6989(00)00240-6.

[15] U. Karsten, Defense strategies of algae and cyanobacteria against solar ultraviolet radiation, in: C.D. Amsler (Ed.), Algal Chem. Ecol., Springer Berlin Heidelberg, Berlin, Heidelberg, 2008, pp. 273–296.

[16] M. Hatakeyama, S. Nakamura, "Button-on-a-string" mechanism in water, the ultrafast UV-to-heat conversion by mycosporine-like amino acid porphyra-334 of natural sunscreen compound, ACS Phys. Chem. Au 5 (3) (2025) 274–282, https://doi.org/10.1021/acsphyschemau.4c00107.

[17] A. Oren, N. Gunde-Cimerman, Mycosporines and mycosporine-like amino acids: UV protectants or multipurpose secondary metabolites? FEMS Microbiol. Lett. 269 (1) (2007) 1–10, https://doi.org/10.1111/j.1574-6968.2007.00650.x.

[18] M. Görünmek, B. Ballık, Z.E. Çakmak, T. Çakmak, Mycosporine-like amino acids in microalgae and cyanobacteria: biosynthesis, diversity, and applications in biotechnology, Algal Res. 80 (2024) 103507, https://doi.org/10.1016/j.algal.2024.103507.

[19] M. Volkmann, A.A. Gorbushina, L. Kedar, A. Oren, Structure of euhalothece-362, a novel red-shifted mycosporine-like amino acid, from a halophilic cyanobacterium (Euhalothece sp.), FEMS Microbiol. Lett. 258 (1) (2006) 50–54, https://doi.org/10.1111/j.1574-6968.2006.00203.x.

[20] N.K. Peinado, R.T. Abdala Díaz, F.L. Figueroa, E.W. Helbling, Ammonium and UV radiation stimulate the accumulation of mycosporine-like amino acids in *Porphyra columbina* (Rhodophyta) from Patagonia, Argentina, J. Phycol. 40 (2) (2004) 248–259, https://doi.org/10.1046/j.1529-8817.2004.03013.x.

[21] D. Joshi, C. Mohandass, M. Dhale, Effect of UV-B radiation and desiccation stress on photoprotective compounds accumulation in marine Leptolyngbya sp, Appl. Biochem. Biotechnol. 184 (1) (2018) 35–47, https://doi.org/10.1007/s12010-017-2523-3.

[22] K. Michalek-Wagner, Seasonal and sex-specific variations in levels of photo-protecting mycosporine-like amino acids (MAAs) in soft corals, Mar. Biol. 139 (4) (2001) 651–660, https://doi.org/10.1007/s002270100625.

[23] R. Waditee-Sirisattha, H. Kageyama, W. Sopun, Y. Tanaka, T. Takabe, Identification and upregulation of biosynthetic genes required for accumulation of mycosporine-2-glycine under salt stress conditions in the halotolerant cyanobacterium Aphanothece halophytica, Appl. Environ. Microbiol. 80 (5) (2014) 1763–1769, https://doi.org/10.1128/AEM.03729-13.

[24] U. Karsten, Effects of salinity and ultraviolet radiation on the concentration of mycosporine-like amino acids in various isolates of the benthic cyanobacterium Microcoleus chthonoplastes, Phycol. Res. 50 (2) (2002) 129–134, https://doi.org/10.1046/j.1440-1835.2002.00266.x.

[25] R.P. Sinha, D.P. Häder, Life under solar UV radiation in aquatic organisms, Adv. Space Res. 30 (6) (2002) 1547–1556, https://doi.org/10.1016/S0273-1177(02)00370-8.

[26] P. Mondal, A. Sen, P. Shaw, A. Dey Bhowmik, S. Mandal, A. Chattopadhyay, et al., UV-absorbing compound asterina-330 mitigates the cytotoxic effect of arsenic and fluoride in zebrafish hepatocytes, Nucleus (2025), https://doi.org/10.1007/s13237-025-00573-y.

[27] J. Ryu, S.J. Park, I.H. Kim, Y.H. Choi, T.J. Nam, Protective effect of porphyra-334 on UVA-induced photoaging in human skin fibroblasts, Int. J. Mol. Med. 34 (3) (2014) 796–803, https://doi.org/10.3892/ijmm.2014.1815.

[28] M. Orfanoudaki, A. Hartmann, M. Alilou, T. Gelbrich, P. Planchenault, S. Derbré, et al., Absolute configuration of mycosporine-like amino acids, their wound healing properties and in vitro anti-aging effects, Mar. Drugs 18 (1) (2020) 35, https://doi.org/10.3390/md18010035.

[29] K. Wang, J. Cao, M. Yao, Q. Zhang, H. Lin, L. Qin, et al., Biosynthesis of the natural antioxidant mycosporine-glycine and its anti-photodamage properties, J. Agric. Food Chem. 73 (18) (2025) 11094–11109, https://doi.org/10.1021/acs.jafc.5c03351.

[30] A. Hartmann, A. Murauer, M. Ganzera, Quantitative analysis of mycosporine-like amino acids in marine algae by capillary electrophoresis with diode-array detection, J. Pharm. Biomed. Anal. 138 (2017) 153–157, https://doi.org/10.1016/j.jpba.2017.01.053.

[31] M. Orfanoudaki, A. Hartmann, U. Karsten, M. Ganzera, Chemical profiling of mycosporine-like amino acids in twenty-three red algal species, J. Phycol. 55 (2) (2019) 393–403, https://doi.org/10.1111/jpy.12827.

[32] E. Angulo-Nuñez, N. Rincón-Díaz, M. Puyana, G. Costa, V. Urrea-Victoria, L. Castellanos, et al., Photoprotective potential of mycosporine-like amino acids in red algae (Rhodophyta) from San Andrés and Providencia Islands, Colombian Caribbean, Rev. Bras. Farmacogn. 35 (4) (2025) 754–762, https://doi.org/10.1007/s43450-025-00663-7.

[33] M. Orfanoudaki, A. Hartmann, H. Miladinovic, H. Nguyen Ngoc, U. Karsten, M. Ganzera, Bostrychines A–F, six novel mycosporine-like amino-acids and a novel betaine from the red alga *Bostrychia scorpioides*, Mar. Drugs 17 (6) (2019) 356, https://doi.org/10.3390/md17060356.

[34] M. Orfanoudaki, A. Hartmann, M. Kamiya, J. West, M. Ganzera, Chemotaxonomic study of *Bostrychia* spp. (Ceramiales, Rhodophyta) based on their mycosporine-like amino acid content, Molecules 25 (14) (2020) 3273, https://doi.org/10.3390/molecules25143273.

[35] M. Orfanoudaki, M. Alilou, A. Hartmann, J. Mayr, U. Karsten, H. Nguyen-Ngoc, et al., Isolation and structure elucidation of novel mycosporine-like amino acids from the two intertidal red macroalgae *Bostrychia scorpioides* and *Catenella caespitosa*, Mar. Drugs 21 (10) (2023) 543, https://doi.org/10.3390/md21100543.

[36] A. Hartmann, K. Becker, U. Karsten, D. Remias, M. Ganzera, Analysis of mycosporine-like amino acids in selected algae and cyanobacteria by hydrophilic interaction liquid chromatography and a novel MAA from the red alga Catenella repens, Mar. Drugs 13 (10) (2015) 6291–6305, https://doi.org/10.3390/md13106291.

[37] M. Zwerger, M. Ganzera, Fast and efficient separation of eleven mycosporine-like amino acids by UHPLC-DAD and their quantification in diverse red algae, Mar. Drugs 20 (6) (2022) 395, https://doi.org/10.3390/md20060395.

[38] M.J. Zwerger, F. Hammerle, B. Siewert, M. Ganzera, Application of feature-based molecular networking in the field of algal research with special focus on mycosporine-like amino acids, J. Appl. Phycol. 35 (3) (2023) 1377–1392, https://doi.org/10.1007/s10811-023-02906-3.

[39] P.-M. Allard, J. Bisson, A. Azzollini, G.F. Pauli, G.A. Cordell, J.-L. Wolfender, Pharmacognosy in the digital era: shifting to contextualized metabolomics, Curr. Opin. Biotechnol. 54 (2018) 57–64, https://doi.org/10.1016/j.copbio.2018.02.010.

[40] L.-F. Nothias, D. Petras, R. Schmid, K. Dührkop, J. Rainer, A. Sarvepalli, et al., Feature-based molecular networking in the GNPS analysis environment, Nat. Methods 17 (9) (2020) 905–908, https://doi.org/10.1038/s41592-020-0933-6.

[41] R. Schmid, D. Petras, L.-F. Nothias, M. Wang, A.T. Aron, A. Jagels, et al., Ion identity molecular networking for mass spectrometry-based metabolomics in the GNPS environment, Nat. Commun. 12 (1) (2021) 3832, https://doi.org/10.1038/s41467-021-23953-9.

[42] R. Bushuiev, A. Bushuiev, R. Samusevich, C. Brungs, J. Sivic, T. Pluskal, Self-supervised learning of molecular representations from millions of tandem mass spectra using DreaMS, Nat. Biotechnol. (2025), https://doi.org/10.1038/s41587-025-02663-3.

[43] F. Huber, S. van der Burg, J.J.J. van der Hooft, L. Ridder, MS2DeepScore: a novel deep learning similarity measure to compare tandem mass spectra, J. Chem. 13 (1) (2021) 84, https://doi.org/10.1186/s13321-021-00558-4.

[44] K. Dührkop, M. Fleischauer, M. Ludwig, A.A. Aksenov, A.V. Melnik, M. Meusel, et al., SIRIUS 4: a rapid tool for turning tandem mass spectra into metabolite structure information, Nat. Methods 16 (4) (2019) 299–302, https://doi.org/10.1038/s41592-019-0344-8.

[45] A. Rutz, M. Dounoue-Kubo, S. Ollivier, J. Bisson, M. Bagheri, T. Saesong, et al., Taxonomically informed scoring enhances confidence in natural products annotation, Front. Plant Sci. 10 (2019) 1329, https://doi.org/10.3389/fpls.2019.01329.

[46] M. Wang, J.J. Carver, V.V. Phelan, L.M. Sanchez, N. Garg, Y. Peng, et al., Sharing and community curation of mass spectrometry data with Global Natural Products Social Molecular Networking, Nat. Biotechnol. 34 (8) (2016) 828–837, https://doi.org/10.1038/nbt.3597.
[47] C. Brungs, R. Schmid, S. Heuckeroth, A. Mazumdar, M. Drexler, P. Šácha, et al., MSnLib: efficient generation of open multi-stage fragmentation mass spectral libraries, Nat. Methods 22 (10) (2025) 2028–2031, https://doi.org/10.1038/s41592-025-02813-0.
[48] M. Volkmann, A.A. Gorbushina, A broadly applicable method for extraction and characterization of mycosporines and mycosporine-like amino acids of terrestrial, marine and freshwater origin, FEMS Microbiol. Lett. 255 (2) (2006) 286–295, https://doi.org/10.1111/j.1574-6968.2006.00088.x.
[49] M. Nothias-Esposito, L.F. Nothias, R.R. Da Silva, P. Retailleau, Z. Zhang, P. Leyssen, et al., Investigation of premyrsinane and myrsinane esters in Euphorbia cupanii and Euphobia pithyusa with MS2LDA and combinatorial molecular network annotation propagation, J. Nat. Prod. 82 (6) (2019) 1459–1470, https://doi.org/10.1021/acs.jnatprod.8b00916.
[50] Z. Zuo, L. Cao, L.-F. Nothias, H. Mohimani, MS2Planner: improved fragmentation spectra coverage in untargeted mass spectrometry by iterative optimized data acquisition, Bioinformatics 37 (Supplement_1) (2021) i231–i236, https://doi.org/10.1093/bioinformatics/btab279.
[51] M.C. Chambers, B. Maclean, R. Burke, D. Amodei, D.L. Ruderman, S. Neumann, et al., A cross-platform toolkit for mass spectrometry and proteomics, Nat. Biotechnol. 30 (10) (2012) 918–920, https://doi.org/10.1038/nbt.2377.
[52] R. Schmid, S. Heuckeroth, A. Korf, A. Smirnov, O. Myers, T.S. Dyrlund, et al., Integrative analysis of multimodal mass spectrometry data in MZmine 3, Nat. Biotechnol. 41 (4) (2023) 447–449, https://doi.org/10.1038/s41587-023-01690-2.
[53] P. Shannon, A. Markiel, O. Ozier, N.S. Baliga, J.T. Wang, D. Ramage, et al., Cytoscape: a software environment for integrated models of biomolecular interaction networks, Genome Res. 13 (11) (2003) 2498–2504, https://doi.org/10.1101/gr.1239303.
[54] A. Schüller, V. Hähnke, G. Schneider, SmiLib v2.0: a java-based tool for rapid combinatorial library enumeration, QSAR Comb. Sci. 26 (3) (2007) 407–410, https://doi.org/10.1002/qsar.200630101.
[55] K. Dührkop, H. Shen, M. Meusel, J. Rousu, S. Böcker, Searching molecular structure databases with tandem mass spectra using CSI:FingerID, Proc. Natl. Acad. Sci. 112 (41) (2015) 12580–12585, https://doi.org/10.1073/pnas.1509788112.
[56] K. Dührkop, L.-F. Nothias, M. Fleischauer, R. Reher, M. Ludwig, M.A. Hoffmann, et al., Systematic classification of unknown metabolites using high-resolution fragmentation mass spectra, Nat. Biotechnol. 39 (4) (2021) 462–471, https://doi.org/10.1038/s41587-020-0740-8.
[57] M. Ludwig, L.-F. Nothias, K. Dührkop, I. Koester, M. Fleischauer, M.A. Hoffmann, et al., Database-independent molecular formula annotation using Gibbs sampling through ZODIAC, Nat. Mach. Intell. 2 (10) (2020) 629–641, https://doi.org/10.1038/s42256-020-00234-6.
[58] S. Hofer, M. Stonig, V. Wally, A. Hartmann, D. Fuchs, M. Hermann, et al., Contradictory effects of chemical filters in UV/ROS-stressed human keratinocyte and fibroblast cells, ALTEX 36 (2) (2019) 231–244, https://doi.org/10.14573/altex.1808201.
[59] M. Zwerger, S. Schwaiger, M. Ganzera, Efficient isolation of mycosporine-like amino acids from marine red algae by fast centrifugal partition chromatography, Mar. Drugs 20 (2) (2022) 106, https://doi.org/10.3390/md20020106.
[60] R.R. da Silva, M. Wang, L.-F. Nothias, J.J.J. van der Hooft, A.M. Caraballo-Rodríguez, E. Fox, et al., Propagating annotations of molecular networks using in silico fragmentation, PLoS Comput. Biol. 14 (4) (2018) e1006089, https://doi.org/10.1371/journal.pcbi.1006089.
[61] Y. Xu, J. Li, H. Mao, W. You, J. Chen, H. Xu, et al., Structural annotation, semi-quantification and toxicity prediction of pyrrolizidine alkaloids from functional food: in silico and molecular networking strategy, Food Chem. Toxicol. 176 (2023) 113738, https://doi.org/10.1016/j.fct.2023.113738.
[62] X. Zheng, P. Xie, A.C. Cai, Y. Jiang, S. Huang, X. Ma, et al., Decoding specificity of cyanobacterial MysDs in mycosporine-like amino acid biosynthesis through heterologous expression in Saccharomyces cerevisiae, ACS Omega 10 (13) (2025) 13664–13673, https://doi.org/10.1021/acsomega.5c01035.
[63] M. Chen, G.M. Rubin, G. Jiang, Z. Raad, Y. Ding, Biosynthesis and heterologous production of mycosporine-like amino acid palythines, J. Org. Chem. 86 (16) (2021) 11160–11168, https://doi.org/10.1021/acs.joc.1c00368.
[64] J. Peng, F. Guo, S. Liu, H. Fang, Z. Xu, T. Wang, Recent advances and future prospects of mycosporine-like amino acids, Molecules 28 (14) (2023) 5588, https://doi.org/10.3390/molecules28145588.
[65] H.W. Kim, M. Wang, C.A. Leber, L.-F. Nothias, R. Reher, K.B. Kang, et al., NPClassifier: a deep neural network-based structural classification tool for natural products, J. Nat. Prod. 84 (11) (2021) 2795–2807, https://doi.org/10.1021/acs.jnatprod.1c00399.
[66] C.M. Leach, Ultraviolet-absorbing substances associated with light-induced sporulation in fungi, Can. J. Bot. 43 (2) (1965) 185–200, https://doi.org/10.1139/b65-024.
[67] B. Rainer, S. Schwaiger, L. Dapra, D. Remias, H. Stuppner, A. Trockenbacher, et al., A novel mycosporin like amino acid in an undescribed alga of the Prasiolaceae family, Planta Med. Int. Open 4 (S 01) (2017) Mo-PO-75, https://doi.org/10.1055/s-0037-1608125.
[68] K.H.M. Cardozo, R. Vessecchi, V.M. Carvalho, E. Pinto, P.J. Gates, P. Colepicolo, et al., A theoretical and mass spectrometry study of the fragmentation of mycosporine-like amino acids, Int. J. Mass Spectrom. 273 (1) (2008) 11–19, https://doi.org/10.1016/j.ijms.2008.02.014.
[69] M. Parailloux, S. Godin, S.C.M. Fernandes, R. Lobinski, Untargeted analysis for mycosporines and mycosporine-like amino acids by hydrophilic interaction liquid chromatography (HILIC)—electrospray Orbitrap MS2/MS3, Antioxidants 9 (12) (2020) 1185, https://doi.org/10.3390/antiox9121185.
[70] V. Hotter, K. Glaser, A. Hartmann, M. Ganzera, U. Karsten, Polyols and UV-sunscreens in the Prasiola-clade (Trebouxiophyceae, Chlorophyta) as metabolites for stress response and chemotaxonomy, J. Phycol. 54 (2) (2018) 264–274, https://doi.org/10.1111/jpy.12619.
[71] A.A. Gorbushina, K. Whitehead, T. Dornieden, A. Niesse, A. Schulte, J.I. Hedges, Black fungal colonies as units of survival: hyphal mycosporines synthesized by rock-dwelling microcolonial fungi, Can. J. Bot. 81 (2) (2003) 131–138, https://doi.org/10.1139/b03-011.
[72] M. Volkmann, K. Whitehead, H. Rütters, J. Rullkötter, A.A. Gorbushina, Mycosporine-glutamicol-glucoside: a natural UV-absorbing secondary metabolite of rock-inhabiting microcolonial fungi, Rapid Commun. Mass Spectrom. 17 (9) (2003) 897–902, https://doi.org/10.1002/rcm.997.
[73] R. Sommaruga, D. Libkind, M. van Broock, K. Whitehead, Mycosporine-glutaminol-glucoside, a UV-absorbing compound of two Rhodotorula yeast species, Yeast 21 (13) (2004) 1077–1081, https://doi.org/10.1002/yea.1148.
[74] G. Martins-Silva, R.S. Barbosa, R.S. Santos, A.C.S.R. de Carvalho, M. Kreusch, A.A. A. Padilla, et al., UV radiation triggers mycosporine-glutaminol-glucoside biosynthesis in Naganishia friedmannii FBU002, a non-pathogenic yeast, J. Appl. Microbiol. 136 (3) (2025), https://doi.org/10.1093/jambio/lxaf047.
[75] M. Wei, X. He, N. Liu, H. Deng, Role of reactive oxygen species in ultraviolet-induced photodamage of the skin, Cell Div 19 (1) (2024) 1, https://doi.org/10.1186/s13008-024-00107-z.
[76] M. Zulfiqar, M.R. Crusoe, B. König-Ries, C. Steinbeck, K. Peters, L. Gadelha, Implementation of FAIR practices in computational metabolomics workflows—a case study, Metabolites 14 (2) (2024) 118, https://doi.org/10.3390/metabo14020118.